Ⅲ．研究成果の刊行物・別刷

Assessment of MEF2A Mutations in Myocardial Infarction in Japanese Patients

Kazuaki Kajimoto, PhD; Keisuke Shioji, MD; Naomi Tago, BS; Hitonobu Tomoike, MD; Hiroshi Nonogi, MD; Yoichi Goto, MD; Naoharu Iwai, MD

Background Recently, a mutation in the human MEF2A gene was reported to be responsible for an autosomal dominant form of coronary artery disease, so the purpose of the present study was to assess the significance of MEF2A mutations in Japanese subjects with myocardial infarction (MI).

Methods and Results The study population consisted of 589 control subjects recruited from the Suita study and 379 subjects with MI. The promoter, all the exons, and 3'-UTR regions of MEF2A were sequenced in 190 subjects with myocardial infarction. We found 2 amino acid length polymorphisms, a 7-amino acid deletion polymorphism, and a nonsense mutation (R447X) in exon 12. The length and deletion polymorphisms did not confer susceptibility to MI. Although the nonsense mutation was detected in 1 subject with MI, and in none of the control subjects, the impact of this mutation does not appear to be great; the subject had the MI while in his 70s, had 2 major risk factors, and no family history of ischemic heart disease.

Conclusion MEF2A polymorphism does not contribute appreciably to MI in the Japanese population. (*Circ J* 2005; **69:** 1192–1195)

Key Words: MEF2A; Myocardial infarction; Polymorphisms

Myocardial infarction (MI) is a multifactorial disease caused by environmental and genetic factors. There is an increasing number of studies that have identified the genes contributing to ischemic heart diseases (IHD)[1–8] and recently, a mutation in the human MEF2A gene was reported as responsible for an autosomal dominant form of coronary artery disease (CAD)[9]. The 7-amino acid deletion disrupts the nuclear localization of the mature protein and reduces MEF2A-induced transcriptional activation[9]. The same authors have reported MEF2A missense mutations in 4 of 207 sporadic CAD cases and estimated that MEF2A mutations contribute to approximately 2% of CAD[10]. On the other hand, Weng et al recently reported a lack of MEF2A mutations in 300 CAD cases[11] so the purpose of the present study was to assess the significance of MEF2A mutations in Japanese subjects with MI.

Methods

Study Population

The control group consisted of 589 subjects recruited from the Suita study who were at least 60 years of age with no cardiovascular disease and no family history IHD. The selection criteria and design of the Suita Study have been described previously[12–14] We excluded young subjects from the control group, because they might develop MI in their 50s and 60s. The MI group consisted of 379 randomly selected inpatients and outpatients with documented MI who were admitted to the Division of Cardiology at the National Cardiovascular Center between May 2001 and April 2003 (MI group)[15] The characteristics of the study

population are shown in Table 1. All subjects gave written informed consent and the present study was approved by the Ethics Committee of the National Cardiovascular Center and by the Committee on Genetic Analysis and Gene Therapy of the National Cardiovascular Center.

DNA Studies

A promoter region and all of the 12 exon regions were sequenced in 190 of the subjects with MI (Fig 1) and we found variations that altered the amino acid sequences in exon 12 only. Next, we sequenced exon 12 in 589 control subjects and the remaining 189 subjects with MI. The variations in exon 12 were all determined by sequencing.

Statistical Analysis

All statistical analyses were performed with the JMP

Table 1 Characteristics of the Study Population

	Control	MI	p-value
n	584	379	
Gender (% male)	49.3	85.5	<0.0001
Age (years)	70.6±0.3	58.0±0.4	<0.0001
BMI (kg/m²)	22.67±0.12	23.83±0.115	<0.0001
TC (mg/dl)	207.7±1.4	199.7±2.3 (n=224)	0.0030
HDL-C (mg/dl)	58.8±0.6	43.0±1.1 (n=194)	<0.0001
Smoking			<0.0001
Current	93	228	
Past	163	74	
Never	328	77	
DM (%)	7.7	38.7	<0.0001
HT (%)	35.5	52.9	<0.0001

Data are mean±standard error. Differences between 2 groups (Control vs myocardial infarction (MI)) were calculated by t-test or χ² analysis.
BMI, body mass index; TC, total cholesterol; HDL-C, high-density lipoprotein cholesterol; DM, diabetes mellitus; HT, hypertension.
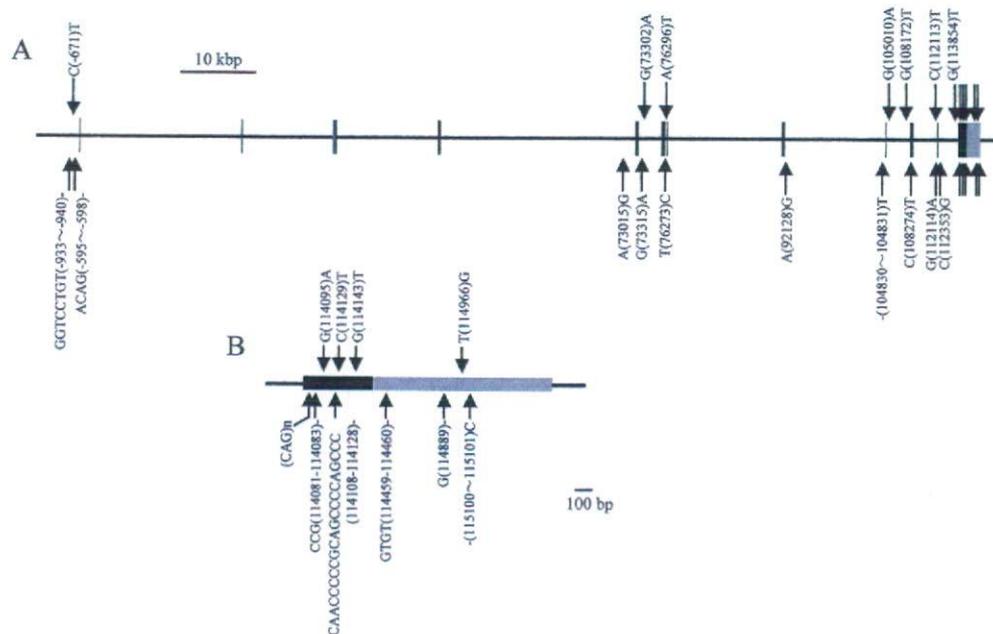
Fig 1. Scheme of the MEF2A gene. (A) Promoter region and all of the 12 exon regions are shown. (B) Expanded region of exon 12. The 5'- and 3'-UTR regions are indicated by gray boxes, and coding regions are indicated by black boxes. The 27 polymorphisms that were found are indicated by arrows.

statistical package (SAS Institute Inc, Cary, NC, USA) unless otherwise stated. Chi-squared analysis was performed to compare haplotype frequencies between the control and MI groups.

Results

We found 27 variations in MEF2A (Table 2), and 4 variations in exon 12 that altered the amino acid sequence of the MEF2A protein (Fig 2). The number of polyglutamine tandem repeats (region A) varied between 4 and 15 (genotype 1), and the number of proline tandem repeats (region B) varied between 4 and 5 (genotype 2). The 21-bp deletion (7-amino acid deletion), which was originally implicated in an autosomal dominant form of CAD[9] was also observed in region C (genotype 3) (Fig 2). We found one nonsense mutation (R447X) in exon 12 in a MI subject, and it was localized just downstream of the 21-bp deletion site (Fig 3).

The haplotype frequencies defined by the 3 genotypes are shown in Table 3: there were no significant differences between the control and MI groups.

Discussion

Wang et al reported that a mutation in the human MEF2A gene was responsible for an autosomal dominant form of CAD[9] but Weng et al could not find any MEF2A mutations in 300 cases of CAD![11] Thus, the association between mutations of MEF2A and CAD is controversial![16,17] and our results favors a lack of association.

Our results indicate that length polymorphisms in MEF2A do not contribute appreciably to MI in the Japanese population. Furthermore, the 21-bp deletion in MEF2A, which was originally implicated[9] did not seem to be associated with MI. The nonsense mutation (R447X) may affect susceptibility to MI, but the particular patient with this mutation had

the MI in his 70 s, and had no family history of IHD. He also had 2 risk factors: diabetes mellitus and smoking. Thus, the impact of this mutation does not appear to be great.

We sequenced all the coding regions of MEF2A in 190 subjects with MI and found neither missense nor nonsense mutations, except for R447X. Taking all our results together, MEF2A polymorphism does not appear to contribute appreciably to MI in the Japanese population.

References

1. Cambien F, Poirier O, Lecerf L, Evans A, Cambou JP, Arveiler D, et al. Deletion polymorphism in the gene for angiotensin-converting enzyme is a potent risk factor for myocardial infarction. *Nature* 1992; **359**: 641–644.
2. Ozaki K, Ohnishi Y, Iida A, Sekine A, Yamada R, Tsunoda T, et al. Functional SNPs in the lymphotoxin-alpha gene that are associated with susceptibility to myocardial infarction. *Nat Genet* 2002; **32**: 650–654.
3. Mukae S, Aoki S, Itoh S, Sato R, Nishio K, Iwata T, et al. Mitochondrial 5178A/C genotype is associated with acute myocardial infarction. *Circ J* 2003; **67**: 16–20.
4. Ozaki K, Inoue K, Sato H, Iida A, Ohnishi Y, Sekine A, et al. Functional variation in LGALS2 confers risk of myocardial infarction and regulates lymphotoxin-alpha secretion in vitro. *Nature* 2004; **429**: 72–75.
5. Ogawa M, Abe S, Biro S. Saigo M, Kihara T, Setoyama S, et al. R353Q polymorphism, activated factor VII, and risk of premature myocardial infarction in Japanese men. *Circ J* 2004; **68**: 520–525.
6. Wang X, Ria M, Kelmenson PM, Eriksson P, Higgins DC, Samnegard A, et al. Positional identification of TNFSF4, encoding OX40 ligand, as a gene that influences atherosclerosis susceptibility. *Nat Genet* 2005; **37**: 365–372.
7. Ozturk O, Ulgen MS, Tekes S, Ozturk U, Toprak N. Influence of

Table 2   The 27 Variations Found in the MEF2A Gene

Region	Polymorphisms	Sequence around polymorphisms	Amino acid mutation
Promoter	GGTCCTGT(−933~−940)−	AGACATTTTAATTTCACCTC[GGTCCTGT/−]GGTCCTGTGGTCCTGTGATC	
	C(−671)T	TGGCCGACGCTTAAGGAAAA[C/T]AGAAAAGAACCTACATGAAT	
	ACAG(−595~−598)−	TTTATTAATGTGAATCATAG[ACAG/−]CCATCAGTCTTCTATTCATT	
Intron 4	A(73015)G	CCTGTAAGTACTTTTACTTT[A/G]CCTCTACTTTTTATTTGTTG	
Intron 5	G(73302)A	GGTGATGACAACAATAAGTA[G/A]AAGGGAAGAAATGCATTTTA	
	G(73315)A	ATAAGTAGAAGGGAAGAAAT[G/A]CATTTTATTAGTATTTTTA	
Intron 6	T(76273)C	CTTTGATGAGCAAGAATCAC[T/C]GATACATAATTGGCCTCATT	
	A(76296)T	TACATAATTGGCCTCATTTT[A/T]AAGTATTTTTTTGAAAATCA	
Intron 8	A(92128)G	GTATTTGAAGAGACAAGTCT[A/G]TTTCAAATACACAAAAATCA	
	−(104830~104831)T	TAGTGTCCAAATATGTTTTT[T/−]CTAAAGAAATATTTTGTTTG	
Intron 9	G(105010)A	CGTGTTGTTATCTAACCAAT[G/A]TTCCCTTTGTTACACAAATT	
	G(108172)T	CAGTGCTTCAGAAAATGACA[T/G]TCATATGAAACTGTGAAAAA	
Exon 10	C(108274)T	TCTTTTTTGATCTCACAGAA[T/C]ACCCAGAGGATCAGTAGTTC	N297N
Intron 10	C(112113)T	AGGAACTTTTGCAGTAGCTA[C/T]GTAAAAAATAGATTCCGTA	
	G(112114)A	GGAACTTTTGCAGTAGCTAC[G/A]TAAAAAATAGATTCCGTATG	
Intron 11	C(112353)G	TTACTCCTGGCCTACACACT[C/G]TCTTTTCCTATCAGTGACAG	
	G(113854)T	CTCTGGGCCCTTTTCCATCA[G/T]GCAGTGTCTCTACTGTATCA	
Exon 12	(CAG)n(n=4–15)(114048–114080)	GTATGACCCCATCGGGCTTC[(CAG)n]CCGCCGCCACCACCGCAGCC	(Q)n (n=4–15)
	CCG(114081–114083)−	AGCAGCAGCAGCAGCAGCAG[CCG/−]CCGCCACCACCGCAGCCA	(P)n (n=4 or 5)
	G(114095)A	CAGCAGCCGCCGCCACCACC[G/A]CAGCCCCAGCCACAACCCCC	P435P
	CAACCCCCGCAGCCCCAGCCC(114108–114128)−	CACCACCGCAGCCCCAGCCA[CAACCCCCGCAGCCCCAGCCC/−]CGACAGGAAATGGGGCGCTC	7 amino acid deletion
Exon 12	C(114129)T	AACCCCCGCAGCCCCAGCCC[C/T]GACAGGAAATGGGGCGCTCC	R447X
	G(114143)T	CAGCCCCGACAGGAAATGGG[G/T]CGCTCCCCTGTGGACAGTCT	G451G
3′-UTR	GTGT(114459–114460)−	ATATATGTATGTGGGTGTGA[-/GTGT]GTGTGTATGTGTGGGTGTGT	
	G(114889)−	AAAACAAACAAAACAAAAAA[G/−]CCCCACACATAACTGTTTTG	
	T(114966)G	TAGCTAATAAAGAAAGAGAA[T/G]AGAAAACACGCATGAGATAT	
	−(115100~115101)C	TCATATCTTAAAAATTAAAG[-/C]AAACTGATTTTAGCTCATGT	

In the polymorphisms found in the exons, mutations of the amino acid sequence are also indicated.

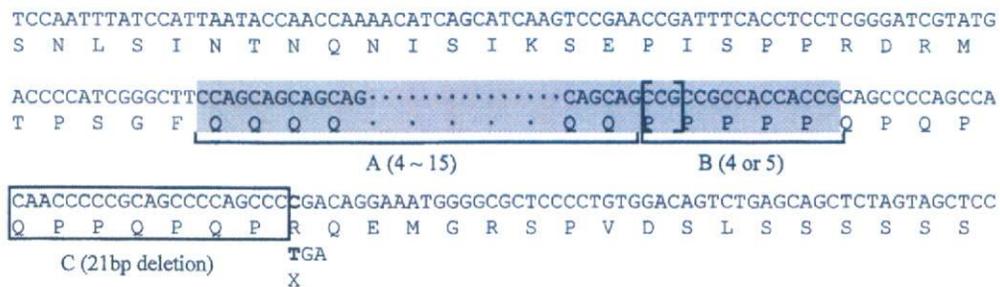Fig 2.   Nucleotide and amino acid sequences of the region containing the 4 variations in exon 12 of MEF2A. The gray box marks the polyglutamine and proline tandem repeats: the number of polyglutamine tandem repeats varies between 4 and 15, the number of proline tandem repeats varies between 4 and 5. The 21-bp deletion site is indicated by a box. The nonsense mutation (R447X) site is localized just downstream to the 21-bp deletion site.

A

B

CAG CCC CAG CCC CGA CAG GAA
Q   P   Q   P   R   Q   E

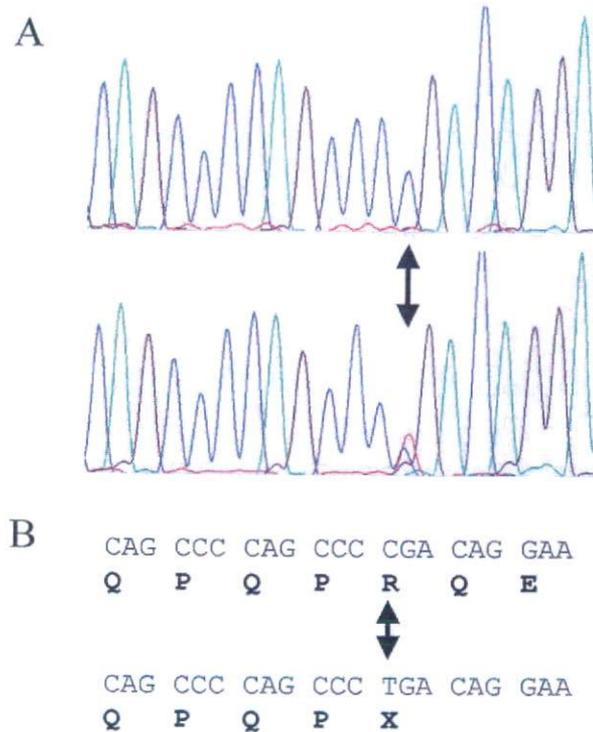CAG CCC CAG CCC TGA CAG GAA
Q   P   Q   P   X

Fig 3. MEF2A nonsense mutation R447X in exon 12 in the subject with myocardial infarction (MI). (A) Sequence analysis of the control and MI subject indicated a C to T substitution at codon 447 in exon 12 of MEF2A. This mutation changes the amino acid residue arginine to stop codon (B).

Table 3 Frequencies of Haplotypes Defined by the 3 Genotypes

Haplotype	C (numbers)	% (row)	MI (numbers)	% (row)
A4B5C+	26	2.23	10	1.32
A5B5C+	2	0.17	5	0.66
A5B4C+	1	0.09	0	0.00
A6B5C+	2	0.17	2	0.26
A7B5C+	5	0.43	2	0.26
A8B5C+	3	0.26	8	1.05
A9B5C+	396	33.90	263	34.61
A9B5C−	3	0.26	3	0.39
A9B4C+	78	6.68	50	6.58
A10B5C+	140	11.99	96	12.63
A10B4C+	0	0.00	2	0.26
A11B5C+	475	40.67	298	39.21
A11B4C+	6	0.51	1	0.13
A12B5C+	5	0.43	6	0.79
A12B4C+	0	0.00	1	0.13
A14B5C+	22	1.88	11	1.45
A15B5C+	4	0.34	2	0.26
	1,168		760	

The frequencies of haplotypes defined by genotypes 1–3 in the control (C) or myocardial infarction (MI) groups are shown. The haplotypes are defined as follows: A represents the number of polyglutamine tandem repeats between 4 and 15 (region A in Fig 2); B represents the number of proline tandem repeats between 4 and 5 (region B); and C+ or − represents the existence or deletion of the 21-bp nucleotide (region C).

angiotensin-converting enzyme I/D gene polymorphism on the right ventricular myocardial performance index in patients with a first acute anterior myocardial infarction. *Circ J* 2005; **69:** 211–215.

8. Momiyama Y, Ohmori R, Nagano M, Kato R, Taniguchi H, Egashira T, et al. Polymorphism of the 3'-untranslated region of interleukin-12 p40 gene is not associated with the presence or severity of coronary artery disease. *Circ J* 2005; **69:** 793–797.

9. Wang L, Fan C, Topol SE, Topol EJ, Wang Q. Mutation of MEF2A in an inherited disorder with features of coronary artery disease. *Science* 2003; **302:** 1578–1581.

10. Bhagavatula MR, Fan C, Shen GQ, Cassano J, Plow EF, Topol EJ, et al. Transcription factor MEF2A mutations in patients with coronary artery disease. *Hum Mol Genet* 2004; **13:** 3181–3188.

11. Weng L, Kavaslar N, Ustaszewska A, Doelle H, Schackwitz W, Hebert S, et al. Lack of MEF2A mutations in coronary artery disease. *J Clin Invest* 2005; **115:** 1016–1020.

12. Mannami T, Konishi M, Baba S, Nishi N, Terao A. Prevalence of asymptomatic carotid atherosclerotic lesions detected by high-resolution ultrasonography and its relation to cardiovascular risk factors in the general population of a Japanese city: The Suita study. *Stroke* 1997; **28:** 518–525.

13. Shioji K, Mannami T, Kokubo Y, Inamoto N, Takagi S, Goto Y, et al. Genetic variants in PCSK9 affect the cholesterol level in Japanese. *J Hum Genet* 2004; **49:** 109–114.

14. Kokubo Y, Iwai N, Tago N, Inamoto N, Okayama A, Yamawaki H, et al. Association analysis between hypertension and CYBA, CLCNKB, and KCNMB1 functional polymorphisms in the Japanese population: The Suita Study. *Circ J* 2005; **69:** 138–142.

15. Shioji K, Mannami T, Kokubo Y, Goto Y, Nonogi H, Iwai N. An association analysis between ApoA1 polymorphisms and the high-density lipoprotein (HDL) cholesterol level and myocardial infarction (MI) in Japanese. *J Hum Genet* 2004; **49:** 433–439.

16. Wang Q, Rao S, Topol EJ. Miscues on the "lack of MEF2A mutations" in coronary artery disease. *J Clin Invest* 2005; **115:** 1399–1400.

17. Weng L, Cohen J, McPherson R, Pennacchio LA. Response to Wang et al. *J Clin Invest* 2005; **115:** 1400.

−20−

Assessment of Genetic Effects of Polymorphisms in the MCP-1 Gene on Serum MCP-1 Levels and Myocardial Infarction in Japanese

Naoharu Iwai, MD*,**; Kazuaki Kajimoto, PhD*; Yoshihiro Kokubo, MD†;
Akira Okayama, MD†; Shunichi Miyazaki, MD**; Hiroshi Nonogi, MD**;
Yoichi Goto, MD**; Hitonobu Tomoike, MD†

Background Recently, the Framingham Heart Study reported that genetic variations in *CCL2* influence serum levels of monocyte chemoattractant protein-1 (MCP-1) and the incidence of myocardial infarction (MI). The purpose of the present study was to investigate the possible involvement of *CCL2* in the pathogenesis of atherosclerosis and MI in Japanese.

Methods and Results Multiple regression analysis indicated that the MCP-1 levels were significantly influenced by various factors including age, body mass index, smoking, alcohol intake, high density lipoprotein-cholesterol, and systolic blood pressure. Moreover, the serum MCP-1 level was significantly correlated with intima–media thickness (p<0.0001). However, this association disappeared when other clinical confounding factors were included in the analyses. Comprehensive analysis of common polymorphisms of *CCL2* in a large community-based population and in subjects with MI found that the A(−2138)T polymorphism affected the serum MCP-1 level in a subgroup of subjects 65 years and older. However, no significant differences in the frequencies of any of the polymorphisms or haplotypes were found between subjects with and without MI. None of the polymorphisms in *CCL2* affected carotid atherosclerosis.

Conclusions The serum MCP-1 level was a good surrogate marker of atherosclerosis in the present study population. Although genetic variations in *CCL2* may have some influence on MCP-1 production, their influence does not seem to contribute appreciably to atherosclerosis in Japanese. The present results did not support the recently published findings from the Framingham Heart Study. The discrepancy between the 2 studies may be related to differences in confounding factors that contribute to MCP-1 levels and in the haplotype structure of the 2 populations. (*Circ J* 2006; **70**: 805–809)

Key Words: Atherosclerosis; Epidemiology; Monocyte chemoattractant protein-1; Myocardial infarction; Polymorphisms

onocyte chemoattractant protein-1 (MCP-1; gene name *CCL2*) has been suggested to play an important role in the initiation of atherosclerosis by recruiting monocytes to sites of injured endothelium. MCP-1 promotes monocyte differentiation to lipid-laden macrophages, and also contributes to the proliferation of arterial smooth muscle cells.[1–4]

In various murine models of atherosclerosis, deletion of *CCL2* has resulted in large reductions in atherosclerotic plaque size[5] but conversely, overexpression of MCP-1 in the leukocytes of susceptible mice resulted in increased plaque size.[6]

Several human epidemiological studies have also suggested links between MCP-1 levels and atherosclerotic disease.[7–10] Higher MCP-1 levels have been associated with increased risks of myocardial infarction (MI), sudden death, coronary angioplasty, and stent restenosis. Very recently, the Framingham Heart Study reported that *CCL2* polymor-

Table 1 Characteristics of the Study Population

	Suita	MI	p value
n	2,266	342	
M (%)	46.0	87.1	<0.0001
Age	65.2 (11.0)	57.9 (9.9)	<0.0001
BMI	22.8 (3.1)	23.9 (2.9)	<0.0001
HTN (%)	38.7	53.4	<0.0001
DM (%)	9.4	40.4	<0.0001
TG	107 (71)	125 (69)*	0.0007
TC	209 (33)	197 (37)*	<0.0001
HDL-C	60 (16)	43 (13)*	<0.0001
Smoking	16.3	61.1	<0.0001
MCP-1	243 (958)**	–	
log (MCP-1)	5.23 (0.42)**	–	
IMT	0.79 (0.13)***	–	
MI	34 (1.5%)	342 (100%)	

Values are expressed as mean (SD).
*n=235, **n=2,180, ***n=2,035.
MI, myocardial infarction; M, male subjects; BMI, body mass index (kg/m²); HTN, hypertensive subjects; DM, diabetes mellitus; TG, triglycerides (mg/dl); TC, total cholesterol (mg/dl); HDL-C, high density lipoprotein cho-lesterol (mg/dl); Smoking, current smokers; MCP-1, serum MCP-1 level (ng/ml); log (MCP-1), logarithmic transformation of MCP-1 level; IMT, intima media thickness (mm).

Table 2 Probes and Primers in TaqMan

| Polymorphisms | Probe | | Primer | |
	VIC	FAM	Forward	Reverse
G(–2581)A	acagctGtcactttc	agacagctAtcactttc	tttccactcacttctctcacgc	gacttggccttttgcatatatcaga
A(–2138)T	ctctctctaatcTgttagtgcat	ctctctctaatcAgttagtgcat	cccgaagcatgactggattat	cctaggccatctcacctcatct
A(–1811)G	aaatggccActccatag	aatggccGctccata	caaagcagggctcgagttg	cctgggactagacttgatgtctca
C(–972)G	ctttagctgtCtgcccat	ttagctgtGtgcccatt	gcctcctaactcataatgacttagcc	ctctgtcctcagcatcttccaa
G(–928)C	aagcaGgcaactagt	ccaagcacgCaacta	tggaagatgctgaggucagaga	ggaaacgtgtacaagtcctccaa
C(7320112)G	atgagctctttCtcttct	tgagctctttGtcttct	tgaggtataggcagaagcactgg	aagcaaaaggcaggcagga

Table 3 Summary of CCL2 Polymorphisms

Polymorphism	Sequence	Region		Mi-AF
G(–2581)A	GACAGCT[G/A]TCACTTT	Promoter		0.332
G(–2411)C	CAAAGCT[G/C]GGAAGTT	Promoter		0.082
A(–2138)T	CACTAAC[T/A]GATTAGA	Promoter		0.049
A(–1811)T	AATGGCC[A/T]CTCCATA	Promoter		0.082
C(–972)G	TAGCTGT[C/G]TGCCCAT	Promoter		0.005
G(–928)C	CCAAGCA[G/C]GCAACTA	Promoter		0.049
C(–362)G	CGCTTCA[C/G]AGAAAGC	Promoter		0.332
C(7320112)G	GCTCTTT[C/G]TCTTCTC	Intron1		0.086
T(7320249)C	CCTGCTG[T/C]TATAACT	Exon2	Cys–>Cys	0.044
C(7320891)T	AGACACC[C/T]TGTTTTA	Exon3	3′–UTR	0.332

Mi-AF (minor allele frequency) was calculated based on the sequencing data of 93 subjects.

phisms are associated with serum MCP-1 levels and MI[11] In genetic association studies, validation in other study populations is very important to confirm that the observed effects are not statistical errors, so the purpose of the present study was to assess the genetic effects of CCL2 polymorphisms on serum MCP-1 levels and atherosclerosis in Japanese subjects.

Methods

Study Population

The selection criteria and design of the Suita study have been described previously[12–14] The genotypes were determined in 2,266 subjects (including 34 MI subjects) recruited from the Suita study between September 2003 and March 2005. Serum MCP-1 levels were measured in 2,180 subjects. The MI group consisted of 342 randomly selected inpatients and outpatients with documented MI who were enrolled in the Division of Cardiology at the National Cardiovascular Center between May 2001 and April 2003[15,16] All the subjects enrolled in the present study gave written informed consent. The present study was approved by the Ethics Committee of the National Cardiovascular Center and by the Committee on Genetic Analysis and Gene Therapy of the National Cardiovascular Center. The characteristics of the study population are shown in Table 1. Subjects with systolic blood pressure (SBP) ≥140 mmHg, diastolic blood pressure ≥90 mmHg, and/or who were taking antihypertensive medication were categorized as having hypertension. Subject with fasting blood glucose ≥126 mg/dl, hemoglobin A1c ≥6.5%, and/or who were being treated for diabetes mellitus was categorized as having the disease.

Fasting serum samples were collected and stored at –80°C. MCP-1 levels were measured in duplicate with a commercially available ELISA kit (R&D Systems, Minneapolis, MN, USA) according to the manufacturer's instructions. The inter- and intra-assay variabilities were 6.3% and 6.2%, respectively. Because the distribution of serum MCP-1 levels was skewed, the values were logarithmically

transformed in the statistical analysis.

The details of the method used for the carotid ultrasonic examination have been reported previously[14] We used a high-resolution B-mode ultrasonic machine with 7.5-MHz transducers, which gave an axial resolution of 0.2 mm. The regions between 30 mm proximal from the beginning of the dilation of the bifurcation bulb and 15 mm distal from the flow divider of both common carotid arteries (CCAs) were scanned. All measurements were made at the time of scanning with the instrument's electronic caliper and were recorded as photocopies. The intima–media thickness (IMT) was measured on a longitudinal scan of the CCA at a point 10 mm proximal from the beginning of the dilation of the bulb.

DNA Study

The promoter (up to –2.8 kb) and exons 1, 2, and 3 (including 3'UTR) regions were sequenced in 93 subjects, which included the top 12 subjects with high serum MCP-1 levels and the bottom 12 subjects with low serum MCP-1 levels. The sequence primers will be provided on request. The genotypes were determined by the TaqMan method (Table 2). The success rate of genotyping was greater than 96%.

Statistical Analysis

Values are expressed as mean ± standard deviation (SD). All statistical analyses were performed with the JMP statistical package (SAS Institute Inc, Cary, NC, USA). Multiple regression analysis was performed to obtain predictors of the serum MCP-1 level and to assess the contribution of polymorphisms of CCL2 to the serum MCP-1 level. Multiple logistic analysis was performed to obtain predictors for MI. Residuals of the serum MCP-1 level and IMT were calculated by adjusting for appropriate confounding factors. R-square values between polymorphisms and haplotype frequencies in the control and MI groups were analyzed using the SNPAlyze Pro statistical package (version 3.2, Dynacom Inc). A statistical power calculation was per-

Table 4 Linkage Disequilibrium Among the Polymorphisms of CCL2

	G(−2581)A	A(−2138)T	A(−1811)T	C(−972)G	G(−928)C	C(7320112)G
G(−2581)A						
A(−2138)T	0.12356					
A(−1811)T	0.16035	0.00565				
C(−972)G	0.02467	0.00086	0.00034			
G(−928)C	0.12411	0.97084	0.00582	0.00089		
C(7320112)G	0.15605	0.00546	0.00716	0.00108	0.00562	

Linkage disequilibrium (LD) among the polymorphisms of CCL2 was calculated from the TaqMan data of the Suita subjects. R-square values between polymorphisms are shown. Tight LD was observed between the A(−2581)T and G(−928)C polymorphisms.

Table 5 Predictors of Serum MCP-1 Level

Predictor	t-ratio	p value
Age	7.9	<0.0001
BMI	−3.21	0.0014
SBP	2.42	0.0155
Alcohol	2.71	0.0067
Smoking	3.36	0.0008
HDL-C	−2.59	0.0096

Predictors of serum MCP-1 levels were identified by multiple regression analysis (n=2,180). Alcohol, ethanol consumption per day (g/day); Smoking, number of cigarettes per day X years.
SBP, systolic blood pressure. See Table 1 for other abbreviations.

Table 6 Predictors of Intima-Media Thickness

Predictor	t-ratio	p value
log (MCP-1)	0.13	0.7191
Age	353.82	<0.0001
SBP	29.67	<0.0001
Sex	33.21	<0.0001
BMI	33.45	<0.0001

n=2,034, F=128.197, p<0.0001.
The serum MCP-1 levels were assessed in 2,034 of the 2,035 subjects assessed by carotid sonography.
See Tables 1,5 for abbreviations.

Table 7 Influence of the Polymorphisms of CCL2 on Serum MCP-1 Level

	AA	Aa	aa	p value
G(−2581)A	0.002 (0.399)	0.004 (0.418)	−0.020 (0.387)	0.692
n	936	961	270	
A(−2138)T	−0.006 (0.402)	0.049 (0.436)	−0.054 (0.211)	0.122 (0.052)
n	1,909	253	7	
A(−1811)T	0.006 (0.407)	−0.031 (0.406)	−0.079 (0.292)	0.268 (0.117)
n	1,839	313	13	
C(−972)G	−0.001 (0.406)	0.045 (0.404)	−	0.409
n	2,111	54		
G(−928)C	−0.006 (0.403)	0.048 (0.430)	−0.054 (0.211)	0.123 (0.052)
n	1,896	262	7	
C(7320112)G	0.004 (0.401)	−0.013 (0.023)	−0.163 (0.108)	0.259 (0.349)
	1,840	311	14	
A(−2138)T Age ≥65 years	−0.012 (0.351)	0.081 (0.462)	−0.051 (0.153)	0.0126 (0.0041)
	1,041	154	4	
G(−928)C Age ≥65 years	−0.012 (0.351)	0.081 (0.500)	−0.051 (0.153)	0.0124 (0.0040)
	1,035	156	4	

Residuals of log (MCP-1) were calculated by adjusting for Age, BMI, SBP, alcohol, smoking, and HDL-C. Values are expressed as mean (SD). p values calculated by grouping AA/Aa + aa are shown in parentheses. The effects of the A(−2138)T and G(−928)C polymorphisms on the MCP-1 level were more significant in subjects aged 65 years and older.
See Tables 1,5 for abbreviations.

formed with the statistical package SamplePower (version 2.0, SPSS, Chicago, IL, USA).

Results

Sequence Analysis of CCL2

Sequence analyses in 93 subjects revealed the existence of 10 polymorphisms (Table 3) of CCL2. The G(−2581)A was in almost complete linkage disequilibrium (LD) with the C(−362)G and C(7320891)T polymorphisms. The A(−1811)G polymorphism was in almost complete LD with the G(−2411)C polymorphism. Thus, the genotypes of the C(−362)G, C(7320891)T, and G(−2411)C polymorphisms were not determined in the present study. Because the polymorphism in exon 2 [T(7320249)C] was synonymous (Cys−>Cys), this polymorphism was also not determined in the present study. The genotypes of the remaining

6 polymorphisms were determined by the TaqMan method in a total of 2,570 subjects. The LD values calculated from R-square values among these SNPs are shown in Table 4.

Clinical Correlates of Serum MCP-1 Level

Multiple regression analysis indicated that the MCP-1 level was significantly influenced by various factors (p< 0.0001, R-square=0.054) including age (p<0.0001), body mass index (BMI; p=0.0014), smoking (p=0.0008), alcohol intake (p=0.0067), high-density lipoprotein cholesterol (p=0.0096), and SBP (p=0.0155) (Table 5).

Many studies have reported that the serum MCP-1 level is an excellent indicator of atherosclerosis and in our study population the serum MCP-1 level significantly correlated with IMT (p<0.0001, R-square=0.009). However, this association disappeared when other clinical confounding factors were included in the multiple regression analyses (Table 6).

Table 8 *CCL2* Polymorphisms and Incidence of MI

	MI (−)			MI			p value
	AA	Aa	aa	AA	Aa	aa	
G(−2581)A (%)	946	966	274	149	176	39	0.2857
	(43.35)	(44.13)	(12.52)	(40.93)	(48.53)	(10.71)	
A(−2138)T (%)	1,931	250	7	218	45	1	0.8686
	(88.25)	(11.43)	(0.32)	(87.36)	(12.36)	(0.27)	[0.6289]
A(−1811)T (%)	1,861	314	14	304	56	5	0.3337
	(85.02)	(14.34)	(0.64)	(83.29)	(15.34)	(1.37)	[0.3999]
C(−972)G (%)	2,130	54		357	7		0.5548
	(97.53)	(2.47)		(98.08)	(1.92)		
G(−928)C (%)	1,918	259	7	319	45	1	0.9578
	(87.82)	(11.86)	(0.32)	(87.40)	(12.33)	(0.27)	[0.8200]
C(7320112)G (%)	1,855	315	14	302	61	2	0.5229
	(84.94)	(14.42)	(0.64)	(82.74)	(16.71)	(0.55)	[0.2880]

Genotype frequencies between subjects with and without MI are shown. p values calculated by grouping AA/Aa + aa are shown in square parentheses.
See Table 1 for abbreviation.

Table 9 Influence of *CCL2* Polymorphisms on IMT

	AA	Aa	aa	p value
G(−2581)A	−0.003 (0.104)	0.001 (0.105)	0.006 (0.115)	0.421
n	865	908	255	
A(−2138)T	0.000 (0.106)	−0.001 (0.103)	0.065 (0.118)	0.319
n	1,784	237	6	(0.958)
A(−1811)T	0.000 (0.105)	0.003 (0.112)	−0.049 (0.068)	0.227
n	1,717	294	12	(0.752)
C(−972)G	0.000 (0.106)	0.000 (0.113)	−	0.964
n	1,970	53		
G(−928)C	0.000 (0.106)	−0.003 (0.103)	0.065 (0.118)	0.291
n	1,771	246	6	(0.802)
C(7320112)G	−0.001 (0.106)	0.005 (0.101)	0.039 (0.159)	0.275
				(0.278)

Residuals of IMT were calculated by adjusting for sex, age, BMI, and SBP. Values are expressed as mean (SD). p values calculated by grouping AA/Aa + aa are shown in parentheses.
See Tables 1,5 for abbreviations.

Table 10 Haplotype Analysis of the 2 Study Populations

Suita	Framingham	G(−2581)A	A(2138)T	A(−1811)G	G(−928)C	C7320112G	MI (−)	MI	Framingham
Haplo1	H1	G	A	A	G	C	65.2	65.0	27.0
Haplo2	H4 + H5	A	A	A	G	C	13.2	10.9	26.9
Haplo3	H6	A	A	G	G	C	7.8	9.0	4.2
Haplo4	−	A	A	A	G	G	7.5	8.7	−
Haplo5	−	A	T	A	C	C	6.1	6.5	−
−	H2	A	T	A	G	G	<0.01	<0.01	20.3
−	H3	A	A	A	C	C	<0.01	<0.01	18.6

Haplotype frequencies in the MI (−) and MI groups were calculated. Haplotype frequencies reported in the Framingham study are also shown for reference.
See Table 1 for abbreviation.

Thus, the serum MCP-1 level was only a surrogate marker of atherosclerosis in the present study population.

Influence of Polymorphisms on Serum MCP-1 Level

Next, we examined the influence of polymorphisms of *CCL2* on residuals of the MCP-1 level after adjusting for the above-mentioned confounding factors (Adj-MCP1) (Table 7). Two polymorphisms, A(−2138)T and G(−928)C, tended to affect Adj-MCP1. The A(−2138)T and G(−928)C polymorphisms were in tight LD (R-square=0.97084) in this study population (Table 4). Interestingly, the influence of these polymorphisms on Adj-MCP1 seemed to be exaggerated in subjects 65 years and older whose MCP-1 levels were significantly higher than those of younger subjects.

Association Study Between CCL2 Polymorphisms and MI

No significant difference was found in the frequencies of any of the polymorphisms between the cases and controls (Table 8). Multiple logistic analyses including age and BMI indicated that none of the polymorphisms contributed to MI. Moreover, none of them affected IMT after adjusting for sex, age, SBP, and BMI (Table 9).

Haplotype Analysis

We constructed haplotypes based on the G(−2581)A, A(−2138)T, A(−1811)T, G(−928)C, and C7320112G polymorphisms and identified 5 common haplotypes that accounted for 99.7% of all haplotypes. The C(−972)G polymorphism was not included because of its low frequency. No significant difference was observed in haplotype fre-

quencies between subjects with and without MI (Table 8).

The haplotype frequencies reported in the Framingham study[11] were significantly different from those in the present study population (Table 10). Although H2 and H3, which accounted for 20.3% and 18.6%, respectively, in the Framingham study, were very rare in this study population, Haplo4 and 5, which were rare in the Framingham study, were common.

Discussion

This report describes a comprehensive analysis of the common polymorphisms of *CCL2* in both a large community-based population and subjects with MI. No significant differences in the frequencies of any of the polymorphisms were found between cases and controls. Moreover, none of the polymorphisms of *CCL2* affected carotid atherosclerosis as assessed by IMT. However, the A(−2136)T and G(−928)C polymorphisms tended to affect the serum MCP-1 level. Although genetic variations in *CCL2* may have some influence on MCP-1 production, their does not seem to contribute appreciably to atherosclerosis in Japanese subjects. Thus, our findings do not support the recently published result from the Framingham Heart Study[11] that genetic variations in *CCL2* significantly influence serum MCP-1 levels and the incidence of MI.

There may be several reasons for this discrepancy. The MCP-1 levels in the Framingham Heart Study were approximately 1.4-fold higher than those in the present study population. Genetic variation might well have an influence under a stimulated state. MCP-1 levels are influenced by various factors, as described in Table 5. It is conceivable that subjects in the Framingham Heart Study may have had higher MCP-1 levels because of stimulation by atherogenic factors that may be more prevalent in Caucasians. Indeed, the influence of genetic variations was more evident in the present study population when the analysis was limited to older subjects who had higher MCP-1 levels (Table 7).

In the Framingham Heart Study, the haplotype H2 was reported to contribute to higher MCP-1 levels, and the frequency of this haplotype was 20.3%![11] It is defined by the (−2138)T and (77320112)G genotypes, and although the A(−2138)T and G(7320112)C polymorphisms were observed in the present study population, the H2 haplotype was not (p<0.01%). This difference in the haplotype structure between Caucasians and Japanese might also contribute to the discrepancy between the 2 studies.

The reported positive association between the A(−2581)T polymorphism and MI in the Framingham Heart Study was based on 1,797 study subjects, including just 107 MI subjects![11] which was insufficient statistical power (p<0.50) to conclude that there was a positive association between the genotype and MI. Moreover, although the H2 haplotype was reported to be associated with the serum MCP-1 level, the H1 haplotype but not the H2 haplotype, was reported to be associated with MI. This inconsistency might also indicate that the Framingham study had insufficient statistical power.

Although the serum MCP-1 level is an excellent indicator of atherosclerosis,[7–10] MCP-1 itself appears to make only a slight contribution to atherosclerosis (Table 6). Thus, it is unlikely that genetic polymorphisms that may only slightly influence the serum MCP-1 level will contribute significantly to the occurrence of MI and atherosclerosis. Our present findings suggest that, although genetic variations in *CCL2* may have some influence on MCP-1 production, their influ-

ence on the incidence of MI is not appreciable in Japanese. The present study also indicates the importance of clarifying the haplotype structure for comparing genetic association studies involving different ethnic backgrounds.

References

1. Yla-Herttuala S, Lipton BA, Rosenfeld ME, Sarkioja T, Yoshimura T, Leonard EJ, et al. Expression of monocyte chemoattractant protein-1 in macrophage-rich areas of human and rabbit atherosclerotic lesions. *Proc Natl Acad Sci USA* 1991; **88:** 5252–5256.
2. Yu X, Dluz S, Graves DT, Zhang L, Antoniades HN, Hollander W, et al. Elevated expression of monocyte chemoattractant protein-1 by vascular smooth muscle cells in hypercholesterolemic primates. *Proc Natl Acad Sci USA* 1992; **89:** 6953–6957.
3. Nelken NA, Coughlin SR, Gordon D, Wilcox JN. Monocyte chemoattractant protein-1 in human atheromatous plaques. *J Clin Invest* 1991; **88:** 1121–1127.
4. Viedt C, Vogel J, Athanasiou T, Shen W, Orth SR, Kubler W, et al. Monocyte chemoattractant protein-1 induces proliferation and interleukin-6 production in human smooth muscle cells by differential activation of nuclear factor-*k*B and activator protein-1. *Arterioscler Thromb Vasc Biol* 2002; **22:** 914–920.
5. Gu L, Okada Y, Clinton SK, Gerard C, Sukhova GK, Libby P, et al. Absence of monocyte chemoattractant protein-1 reduces atherosclerosis in low density lipoprotein receptor-deficient mice. *Mol Cell* 1998; **2:** 275–281.
6. Aiello RJ, Bourassa PA, Lindsey S, Weng W, Natoli E, Rollins BJ, et al. Monocyte chemoattractant protein-1 accelerates atherosclerosis in apolipoprotein E-deficient mice. *Arterioscler Thromb Vasc Biol* 1999; **19:** 1518–1525.
7. de Lemos JA, Morrow DA, Sabatine MS, Murphy SA, Gibson CM, Antman EM, et al. Association between plasma levels of monocyte chemoattractant protein-1 and long-term clinical outcomes in patients with acute coronary syndromes. *Circulation* 2003; **107:** 690–695.
8. Cipollone F, Marini M, Fazia M, Pini B, Iezzi A, Reale M, et al. Elevated circulating levels of monocyte chemoattractant protein-1 in patients with restenosis after coronary angioplasty. *Arterioscler Thromb Vasc Biol* 2001; **21:** 327–334.
9. Oshima S, Ogawa H, Hokimoto S, Nakamura S, Noda K, Saito T, et al. Plasma monocyte chemoattractant protein-1 antigen levels and the risk of restenosis after coronary stent implantation. *Jpn Circ J* 2001; **65:** 261–264.
10. Deo R, Khera A, McGuire DK, Murphy SA, de PMNJ, Morrow DA, et al. Association among plasma levels of monocyte chemoattractant protein-1, traditional cardiovascular risk factors, and subclinical atherosclerosis. *J Am Coll Cardiol* 2004; **44:** 1812–1818.
11. McDermott DH, Yang Q, Kathiresan S, Cupples LA, Massaro JM, Keaney JF Jr, et al. CCL2 polymorphisms are associated with serum monocyte chemoattractant protein-1 levels and myocardial infarction in the Framingham Heart Study. *Circulation* 2005; **112:** 1113–1120.
12. Kokubo Y, Iwai N, Tago N, Inamoto N, Okayama A, Yamawaki H, et al. Association analysis between hypertension and *CYBA, CLCNKB,* and *KCNMB1* functional polymorphisms in the Japanese population: The Suita study. *Circ J* 2005; **69:** 138–142.
13. Iwai N, Katsuya T, Mannami T, Higaki J, Ogihara T, Kokame K, et al. Association between SAH, an acyl-CoA synthetase gene, and hypertriglyceridemia, obesity, and hypertension. *Circulation* 2002; **105:** 41–47.
14. Mannami T, Konishi M, Baba S, Nishi N, Terao A. Prevalence of asymptomatic carotid atherosclerotic lesions detected by high-resolution ultrasonography and its relation to cardiovascular risk factors in the general population of a Japanese city: The Suita study. *Stroke* 1997; **28:** 518–525.
15. Kajimoto K, Shioji K, Ishida C, Iwanaga Y, Kokubo Y, Tomoike H, et al. Validation of the association between the gene encoding 5-lipoxygenase-activating protein and myocardial infarction in a Japanese population. *Circ J* 2005; **69:** 1029–1034.
16. Kajimoto K, Shioji K, Tago N, Tomoike H, Miyazaki S, Nonogi H, et al. Assessment of MEF2A mutations in myocardial infarction in Japanese patients. *Circ J* 2005; **69:** 1192–1195.

Mechanisms Underlying Nano-Sized Air-Pollution-Mediated Progression of Atherosclerosis

—— Carbon Black Causes Cytotoxic Injury/Inflammation and Inhibits Cell Growth in Vascular Endothelial Cells ——

Hideyuki Yamawaki, PhD; Naoharu Iwai, MD

Background Epidemiological studies indicate a significant link between exposure to environmental air pollution and mortality and morbidity from ischemic heart disease. Because nanoparticles can translocate into blood circulation, the present study aimed to clarify their direct effects on human vascular endothelial cells (ECs).
Methods and Results Human umbilical vein ECs (HUVECs) were treated with carbon black (CB), a component of diesel exhaust particles, for 24 h. CB induced cytotoxic morphological changes such as cytosolic vacuole formation, cell disorientation and decreased density. Lactate dehydrogenase assay revealed that CB induced cytotoxic injury in both the cells and plasma membranes. Proliferation assay showed that CB inhibited cell growth. Monocyte chemoattractant protein-1 but not vascular cell adhesion molecule-1 was induced by CB. CB reduced the expressions of connexin37 and endothelial nitric oxide (NO) synthase. Microarray analysis revealed the induction of pro-inflammatory molecules by CB.
Conclusions The present results demonstrate for the first time that CB directly affects the endothelium, causing cytotoxic injury, inflammatory responses, and inhibition of cell growth. As EC injury/inflammation and membrane disintegration are related to the initiation of atherosclerosis, and NO is anti-atherogenic and anti-thrombogenic, the direct effects of nanoparticles on ECs may represent one mechanism behind environmental air pollution-mediated atherosclerosis and ischemic heart disease. (*Circ J* 2006; **70**: 129–140)

Key Words: Air pollution; Atherosclerosis; Cell death; Endothelium; Inflammation

According to epidemiological studies in the United States and Europe[1,2] modest rises in the mass of particulate matter (PM) are associated with increases in hospitalizations and mortality because of cardiovascular diseases. The absolute number of deaths attributable to PM is much higher for cardiovascular than for respiratory causes[3,4] Traffic-derived nano-sized particles are most likely responsible for the cardiovascular effects because of their larger surface area, potentially leading to the enhanced biological toxicity[5]

Several mechanisms have been proposed; for example, inhaled particles accumulating in the lungs may cause systemic inflammation via oxidative stress, which mediates endothelial dysfunction and atherosclerosis[1,6] The systemic inflammation may also increase blood coagulability by activating platelets and coagulation factors such as fibrinogen[1,6] In addition, some of the cardiovascular effects of PM involve enhancement of autonomic nervous systems via pulmonary reflexes, leading to the arrhythmia[1,7] However, these mechanisms have not been precisely examined.

More recently, Nemmar et al demonstrated that nano-sized particles translocate from the lungs into the blood[1,8,9] and these particles are barely recognized by phagocytosing cells, such as macrophages, compared with micro-sized particles[5] Therefore, because of the low uptake by macrophages, nanoparticles appear to be taken up by epithelial or endothelial cells (ECs) and thus may directly interact with ECs to induce injury and inflammation, promote thrombosis and destabilize atheromatous plaques. However, the effects on vascular ECs have not been precisely examined and so the present study focused particularly on the direct effects of traffic-derived nanoparticles on cultured vascular ECs in order to explore the cellular mechanisms responsible for air pollution-mediated cardiovascular diseases. This study is relevant given that exposure to nano-materials is rapidly increasing, with benefits to medicine from nano-technology such as imaging and drug delivery[5,10]

Methods

Materials

Carbon black (CB; The Association of Powder Process Industry and Engineering, Japan) was suspended in culture medium by sonication and vortexing. CB is a mimetic of soot-like PM derived from the incomplete combustion of diesel engines. Particle size was measured by a Particle Size Analyzer (UPA-EX150, Nikkiso, Japan), revealing a mean diameter±SD of 248.2±161.4 nm (50% accumulation, Fig 1). Antibody sources were as follows: eNOS, VCAM-1, and total actin (Santa Cruz Biotech, CA, USA); proliferating cell nuclear antigen (PCNA: BD Bioscience, CA, USA); and connexin37 (Alpha Diagnostica, TX, USA).
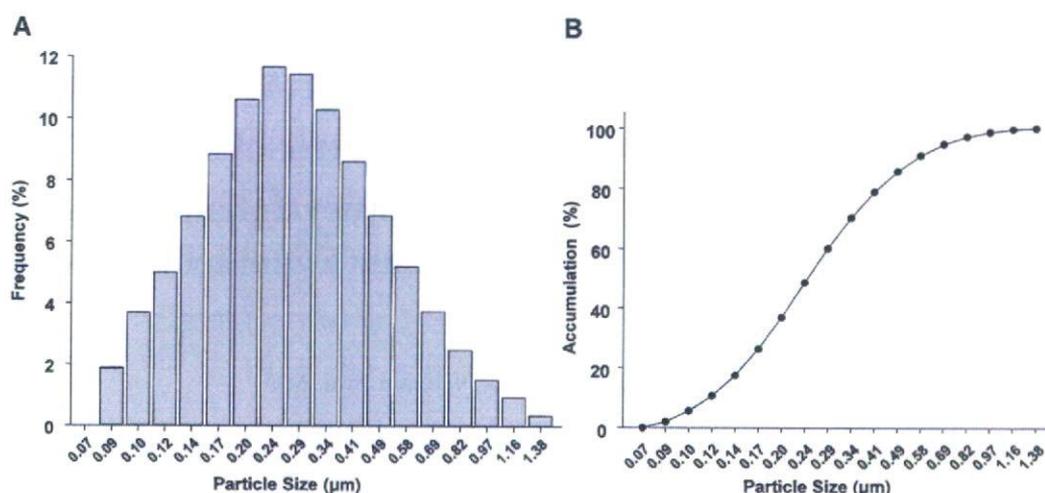
A

B

Fig 1.   Particle size of carbon black suspended in culture medium. (A) Frequency. (B) accumulation.

Cell Culture

Human umbilical vein ECs (HUVECs) were purchased from Cascade Biologics and cultured in Medium 200 supplemented with low serum growth supplement (LSGS; Cascade Biologics, OR, USA) as described previously![1] Cells at passages 3–6 were used for experiments.

Electron Microscopy

HUVECs in 60-mm dishes were fixed in 0.1 mol/L sodium cacodylate-buffered (pH7.4) 2.0% glutaraldehyde solution at 4°C overnight and postfixed in 0.1 mol/L sodium cacodylate-buffered (pH7.4) 1% OsO₄ solution at 4°C for 2h. After dehydration in an ethanol gradient (50–100% each 10min), samples were embedded in EPON812 at 60°C for 2 days. Ultrathin sections (80nm) were stained with uranyl acetate and lead citrate. Sections were examined in a JEOL JEM2000EX at 100kV.

Cytotoxicity Assay

The cytotoxicity assay was performed using a CytoTox 96 non-radioactive cytotoxicity assay kit (Promega, WI, USA) in accordance with the manufacturer's instructions. Briefly, after treating HUVECs at approximately 90% confluence in 6-well plates with CB (1–100μg/ml) for 24h, the culture medium was collected and the level of lactate dehydrogenase (LDH), a stable cytosolic enzyme that is released during cell lysis, was measured at absorbance 490nm using a standard 96-well plate reader. Maximal LDH release was assessed by freeze–thaw lysis of cells, and cytotoxicity was expressed relative to this maximal LDH release.

Proliferation Assay

The proliferation assay was performed using a Cell Counting-8 Kit (Dojindo Laboratories, Japan) according to the manufacturer's instructions. Briefly, after treating HUVECs at approximately 30% confluence in 12-well plates with CB (1–100μg/ml) for 24h, water-soluble tetrazolium salt (WST-8) was added for 3h and the culture medium was collected. Conversion of tetrazolium salt into formazan by living cells (active mitochondria) was measured using a standard 96-well plate reader at absorbance 450nm. The total number of living cells was shown relative to an untreated control sample.

Western Blotting

Western blotting was performed as described previously![2] Proteins were obtained by homogenizing HUVECs with Triton-based lysis buffer (1% Triton X-100, 20mmol/L Tris, pH7.4, 150mmol/L NaCl, 1mmol/L EDTA, 1mmol/L EGTA, 2.5mmol/L sodium pyrophosphate, 1mmol/L β-glycerol phosphate, 1mmol/L Na₃VO₄, 1μg/ml leupeptin, and 0.1% protease inhibitor mixture; Nacalai Tesque, Japan). Protein concentration was determined using the bicinchoninic acid method (Pierce, IL, USA). Equal amounts of proteins (15μg) were separated by SDS-PAGE (7.5%) and transferred to a nitrocellulose membrane (Pall Corporation, MI, USA). After blocking with 5% bovine serum albumin, membranes were incubated with primary antibody (1:1,000 dilution) at 4°C overnight, and membrane-bound antibodies were visualized using horseradish peroxidase-conjugated secondary antibodies (1:10,000 dilution, 1h) and the ECL system (Amersham Biosciences, UK). The resulting autoradiograms were analyzed using NIH Image 1.63 software. Experiments were performed at least 3 times and equal loading of protein was ensured by measuring total actin expression.

Quantitative Determination of Monocyte Chemoattractant Protein (MCP)-1 Release

The MCP-1 protein level was measured using an ELISA kit (Biosource, CA, USA) in accordance with the manufacturer's instructions. Briefly, after treating HUVECs at approximately 90% confluence in 6-well plates with CB (100μg/ml) for 24h, the culture medium was collected and the level of MCP-1 was measured at absorbance 450nm using a standard 96-well plate reader.

Microarray Analysis

Total RNA was isolated from HUVECs treated with or without CB (100μg/ml, 24h) using RNeasy Kit (QUIAGEN Inc, CA, USA) according to the manufacturer's instructions. Only samples with an A260/A280 between 1.7 and 2.2 (measured in 10mmol/L Tris-HCl, pH7.6) were considered suitable for use. Hybridization samples were prepared according to the GeneChip Expression Analysis Technical Manual, 701021 Rev.5 (Section 2: Eukaryotic Sample and Array Processing, Chapter 1: Eukaryotic Target Preparation; http://www.affymetrix.com/support/technical/manuals.affx).
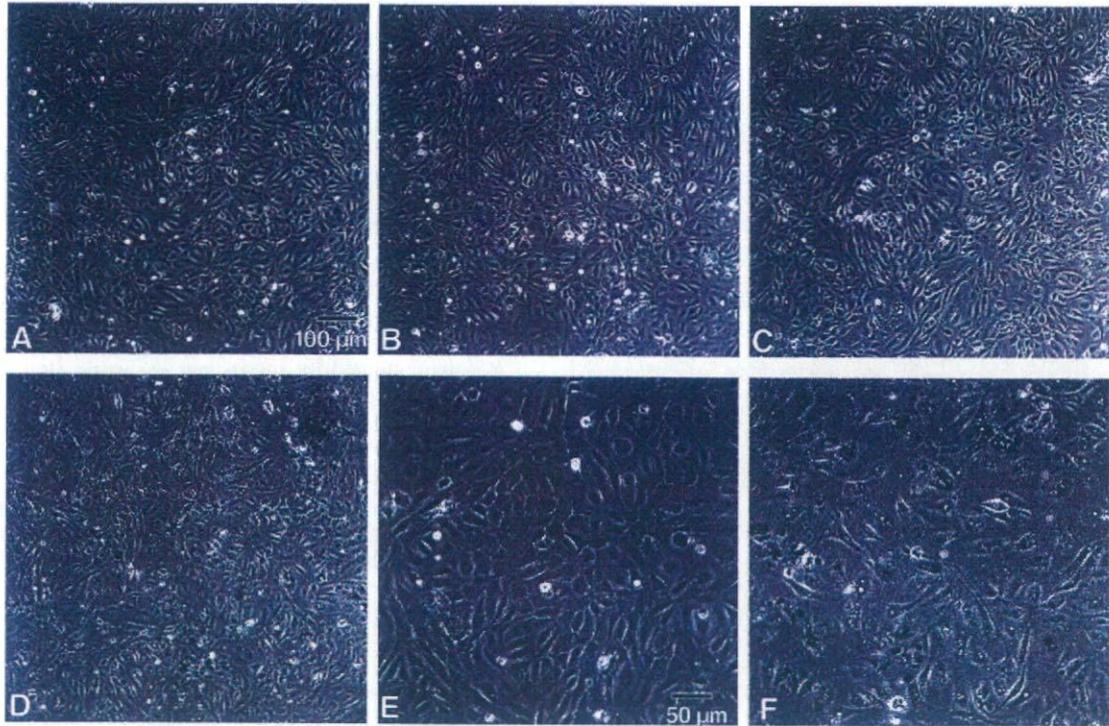
Fig 2. Representative photomicrographs of human umbilical vein endothelial cells (HUVECs) treated with carbon black (CB). HUVECs at ~90% confluence were treated with CB (A,E: $0\,\mu g/ml$; B: $1\,\mu g/ml$; C: $10\,\mu g/ml$; D,F: $100\,\mu g/ml$) for 24 h. Scale bar: $100\,\mu m$ (A–D) and $50\,\mu m$ (E,F).
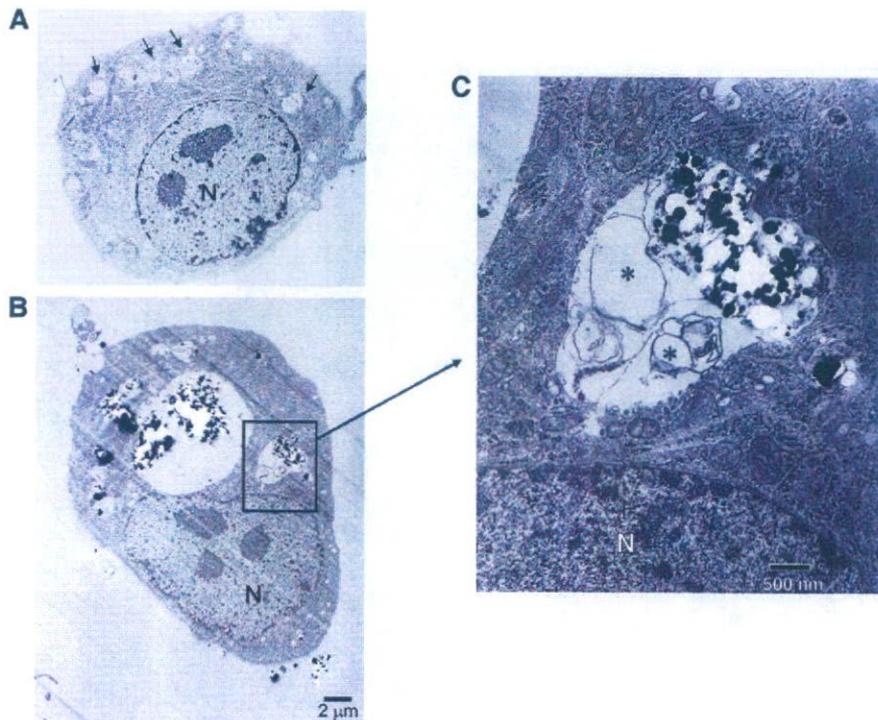
Fig 3. Ultrastructural features of human umbilical vein endothelial cells (HUVECs) treated with carbon black (CB). HUVECs were treated without (A, control) or with $100\,\mu g/ml$ CB (B, C) for 24 h. Arrows, autophagic vacuoles; (*) membranous whorls. N, nucleus. Scale bar: $2\,\mu m$ (A,B) and $500\,nm$ (C).

Total RNA ($2\,\mu g$) was amplified for each sample; cRNA ($30\,\mu g$) was fragmented in $40\,\mu l$ of $1\times$ fragmentation buffer. Hybridization cocktails were made as described in the GeneChip Expression Analysis Technical Manual, 701021 Rev.5 (Section 2, Chapter 2: Eukaryotic Target Hybridiza-

tion) and hybridized to Human genome U133 plus2.0 chips at 60 rpm, 45°C for 16 h using the Hybridization Oven 640 110 V (Affymetrix 800138). The Human genome U133 plus2.0 chips comprise 54,000 probe sets and provide comprehensive coverage of the transcribed human genome on a

Fig 4. Carbon black (CB) induced cytotoxic injury in human umbilical vein endothelial cells (HUVECs) in a dose-dependent manner. HUVECs at ~90% confluence were treated with CB (1–100 $\mu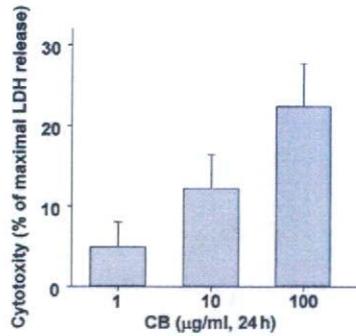$g/ml) for 24 h. Lactate dehydrogenase (LDH) released into supernatant was measured and maximal LDH release was assessed by freeze–thaw lysis of cells. Cytotoxicity was expressed relative to maximal LDH release (n=6–8).

single array to analyze the expression level of more than 47.000 transcripts and variants, including 38,500 well-characterized human genes plus approximately 6,500 new genes. GeneChips were stained with streptavidin-phycoerythrin using the Fluidics Station 450 (Affymetrix 00-0079). After extensive washing, GeneChips were scanned using a GeneChip Scanner 3000 (Affymetrix 00-0074) and the data were analyzed using the GeneChip Operating Software version 1.1 (Affymetrix 690036) according to the GeneChip Expression Analysis Data Analysis Fundamentals (Chapter

4: First-Order Data Analysis and Data Quality Assessment and Chapter 5: Statistical Algorithms Reference; http://www.affymetrix.com/support/technical/manuals.affx). To allow comparison, all chips were scaled to a target intensity of 500 based on all probe sets on each chip. Comparison of the GeneChip array data was obtained using the KURABO custom analysis services (KURABO Industries Ltd, Osaka, Japan, the authorized service provider of Affymetrix Japan K.K., Tokyo, Japan). Hierarchical cluster analysis was performed using Avadis Software version 3.3 for Windows (proprietary product of Strand Genomics Pvt. Ltd, Bangalore, India). Genes that were significantly upregulated by more than 2-fold (top 89 genes, Table 1, Fig 9A) or downregulated by more than −0.5-fold (top 99 genes, Table 2, Fig 9B) in 2 independent experiments are summarized.

Statistical Analysis

Data are shown as mean ± SEM. Statistical evaluations were performed using unpaired Student's t-test and values of p<0.05 were considered statistically significant.

Results

Effects of CB on HUVECs

Cytotoxic Morphological Changes   To examine the direct effects of environmental air pollution on vascular ECs, cultured HUVECs were treated with CB (1–100 μg/ml) for 24 h. This induced cytotoxic morphological changes such as cytosolic vacuole formation, cell disorientation, and
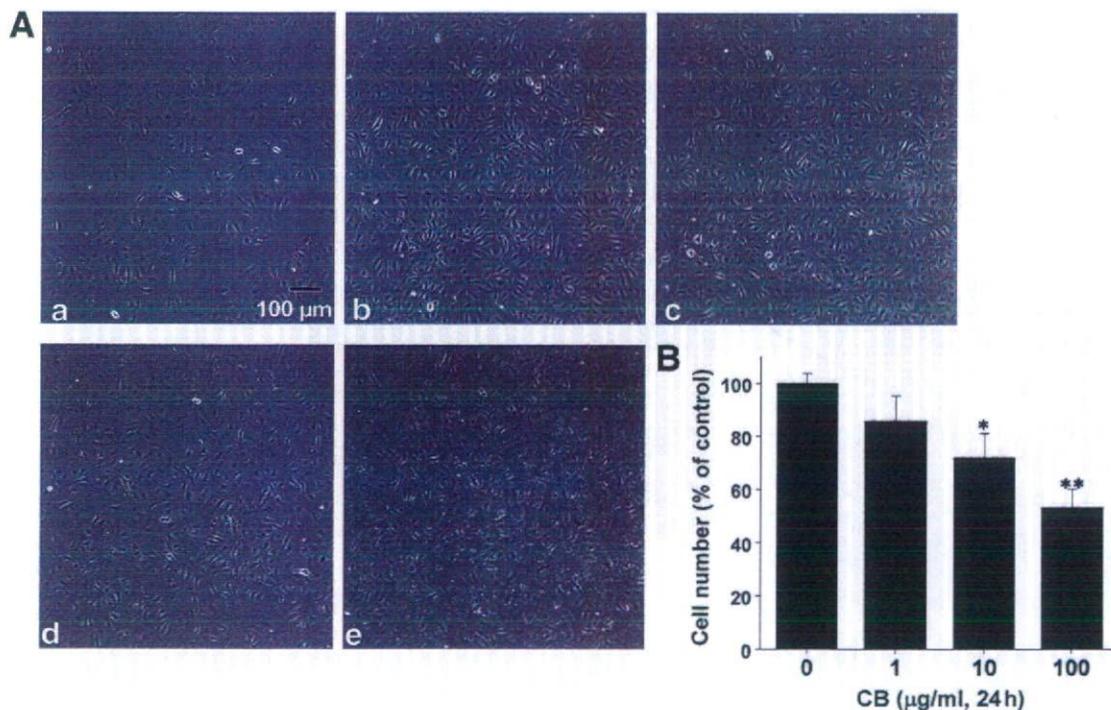
Fig 5. Carbon black (CB) inhibited cell growth in a dose-dependent manner. Human umbilical vein endothelial cells (HUVECs) at ~30% confluence were treated with CB (1–100 μg/ml) for 24 h. (A) Representative photomicrographs of CB for 24 h (a: at start; b: 0 μg/ml; c: 1 μg/ml; d: 10 μg/ml; e: 100 μg/ml). Scale bar: 100 μm (B) Total number of living cells was counted using water-soluble tetrazolium salt (WST-8). Results are shown as percentage relative to control (n=4). *p<0.05 and **p<0.01 compared with control.

A

PCNA

Cont 10 100

CB (µg/ml)

actin

B

Relative Intensity

**

1.0
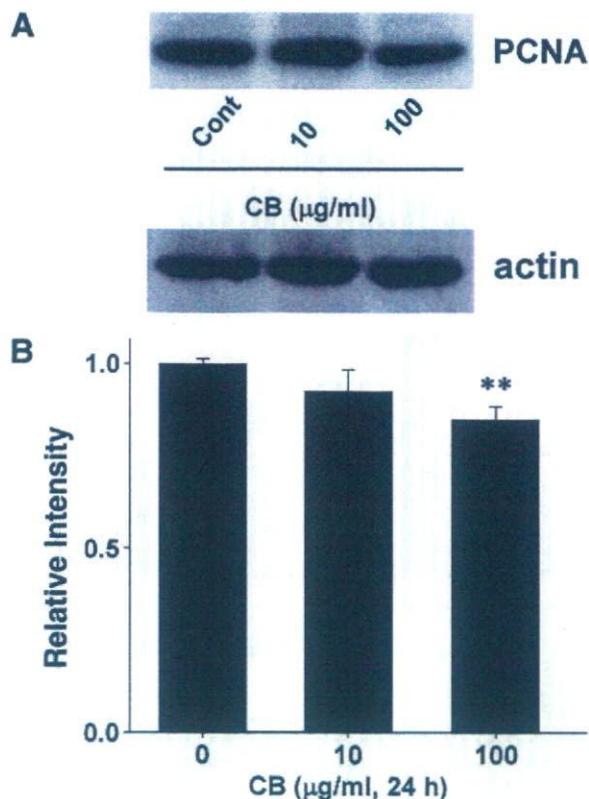
0.5

0.0

0 10 100

CB (µg/ml, 24 h)

Fig 6. Carbon black (CB) inhibited expression of proliferation marker in human umbilical vein endothelial cells (HUVECs). After HUVECs at ~30% confluence were treated with CB (0, 10 or 100 µg/ml) for 24 h, total cell lysates were harvested. (A) Proliferating cell nuclear antigen (PCNA) expression determined by Western blotting. Equal protein loading was confirmed based on total actin antibody. (B) PCNA expression is shown as the fold-change relative to control (n=7–13). **p<0.01 compared with control.

A

MCP-1 (pg/ml)

**

400

300

200

100

0

Cont CB
(100 µg/ml, 24 h)

B
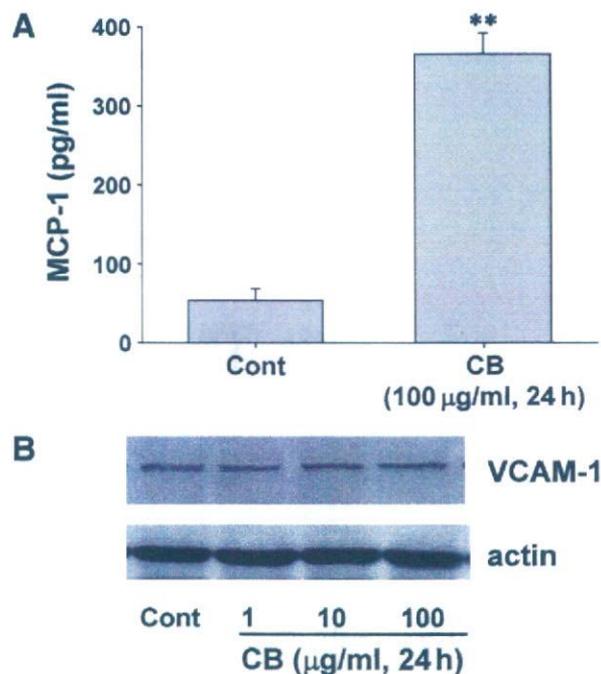
VCAM-1

actin

Cont 1 10 100

CB (µg/ml, 24 h)

Fig 7. Carbon black (CB) increased proinflammatory chemokine but not leukocyte adhesion molecule in human umbilical vein endothelial cells (HUVECs). After HUVECs at ~90% confluence were treated with CB (1–100 µg/ml) for 24 h, (A) culture medium and (B) total cell lysates were harvested. (A) Monocyte chemoattractant protein (MCP)-1 released into supernatant was measured and its concentration expressed as pg/ml. **p<0.01 compared with control (n=5). (B) Vascular cell adhesion molecule (VCAM)-1 expressions determined by Western blotting. Equal protein loading was confirmed using total actin antibody (n=4).

decreased density in a dose-dependent manner (Fig 2A–F). We next performed an ultrastructural analysis using transmission electron microscopy. The cytoplasm of non-treated HUVECs (control; Fig 3A) contained a number of organelles and small vesicles. It has been reported that in vascular smooth muscle cells the formation of small vesicles occurs under normal physiological conditions for the removal of abnormal proteins and other cytoplasmic macromolecules[13] Treatment of HUVECs with CB (100 µg/ml, 24 h) caused extensive vacuolization and internalization of CB (Fig 3B), mainly within autophagic vacuoles, which contained membranous whorls (Fig 3C). Of note, there were a number of CB particles less than 100 nm within the vacuoles.

Increased Release of LDH To quantitatively assess EC injury by CB, we measured endothelial LDH release, a marker of cell death and injury of the plasma membrane. Treatment of HUVECs with CB (1–100 µg/ml, 24 h) increased LDH release into culture medium in a dose-dependent manner (Fig 4; 5.3±3.1% at 1 µg/ml, 12.2±4.2% at 10 µg/ml, and 22.4±5.3% at 100 µg/ml; n=6–8).

Antiproliferative Effects To examine the effects of CB on cell growth, HUVECs at approximately 30% confluence were treated with CB (1–100 µg/ml) for 24 h and then the total number of living cells was measured using WST-8. HUVECs growth was inhibited in a dose-dependent manner (Fig 5A). Quantitative analysis (Fig 5B) revealed that

cell growth was significantly inhibited from 28.0±9.3% (10 µg/ml CB, n=4, p<0.05) to 46.7±7.0% (100 µg/ml CB, n=4, p<0.01). We next examined the effects of CB on the expression of PCNA, which is specifically expressed in the S phase of the cell cycle[14] Western blotting showed that PCNA expression was significantly suppressed by 100 µg/ml CB compared with controls (Fig 6A,B; 15.0± 3.5% inhibition, n=13, p<0.01).

Increased Level of Pro-Inflammatory Chemokines We next examined the effects of CB on the expressions of proinflammatory molecules, because in addition to EC injury, inflammation is another key initiating process for atherosclerosis. MCP-1, acting through its receptor CCR2, appears to play an early and important role in the recruitment of monocytes to atherosclerotic lesions[15] and it has been suggested that the serum concentration of MCP-1 is an independent risk factor for progression of atherosclerosis[16] CB (100 µg/ml, 24 h) significantly increased the production of MCP-1 in HUVECs (Fig 7A, 55.1±14.2 pg/ml in control vs 366.0±26.0 pg/ml in CB, n=5, p<0.01). Vascular cell adhesion molecule (VCAM)-1 participate in the recruitment of leukocytes by inducing their firm adhesion to the activated endothelium[17] Western blotting revealed that the expression levels of VCAM-1 were similar between the controls and CB-treated HUVECs (Fig 7B, n=4).

Suppression of Expressions of Gap Junctions and Endothelial NO Synthase (eNOS) Because impairment of the membrane permeability of ECs is crucial for the initiation of atherosclerosis[18,19] the effects of CB on the expression
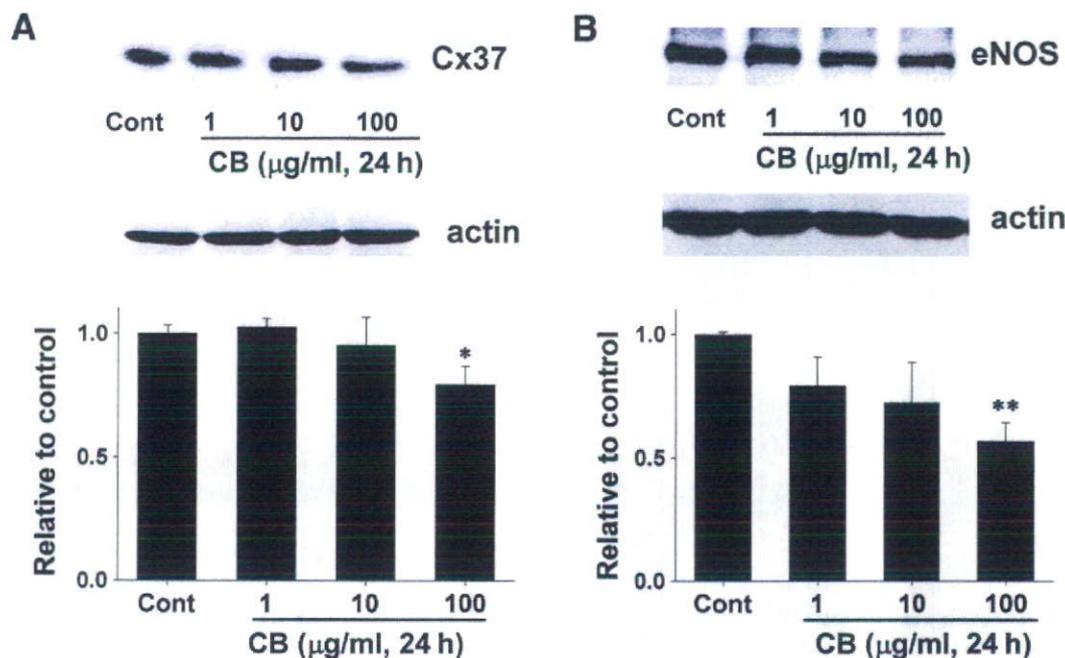
YAMAWAKI H et al.

A

B

Fig 8. Carbon black (CB) inhibited expressions of connexin37 (Cx37) and endothelial nitric oxide synthase (eNOS) in human umbilical vein endothelial cells (HUVECs). After HUVECs at ~90% confluence were treated with CB (1–100 μg/ml) for 24 h, total cell lysates were harvested. (A) Cx37 and (B) eNOS expressions were determined by Western blotting. Equal protein loading was confirmed using total actin antibody. Expression is shown as the fold-change relative to control (n=4–6 (A) and n=3–5 (B)). *p<0.05 and **p<0.01 compared with control.

Table 1 List of Top 89 Probe Sets Upregulated by Carbon Black (CB) Identified on U133 Chips

Probe set ID	GenBank accession	Gene symbol	Gene name	Ratio 1 (fold)	Ratio 2 (fold)
200939_s_at	NM_012102	RERE	Arginine-glutamic acid dipeptide (RE) repeats	2.08	3.23
201566_x_at	D13891	ID2	Inhibitor of DNA binding 2, dominant negative helix-loop-helix protein	2.25	2.39
202637_s_at	AI608725	ICAM1	Intercellular adhesion molecule 1 (CD54), human rhinovirus receptor	5.29	2.13
202638_s_at	NM_000201	ICAM1	Intercellular adhesion molecule 1 (CD54), human rhinovirus receptor	5.20	5.33
202672_s_at	NM_001674	ATF3	Activating transcription factor 3	3.02	4.85
202768_at	NM_006732	FOSB	FBJ murine osteosarcoma viral oncogene homolog B	28.41	8.97
202859_x_at	NM_000584	IL8	Interleukin 8	2.29	2.34
203665_at	NM_002133	HMOX1	Heme oxygenase (decycling) 1	4.13	2.31
203868_s_at	NM_001078	VCAM1	Vascular cell adhesion molecule 1	3.96	5.39
204114_at	NM_007361	NID2	Nidogen 2 (osteonidogen)	2.04	2.20
204472_at	NM_005261	GEM	GTP binding protein overexpressed in skeletal muscle	4.28	4.84
204595_s_at	AI300520	STC1	Stanniocalcin 1	2.57	2.27
204622_x_at	NM_006186	NR4A2	Nuclear receptor subfamily 4, group A, member 2	13.88	4.12
204698_at	NM_002201	ISG20	Interferon stimulated gene 20 kDa	3.76	4.06
204748_at	NM_000963	PTGS2	Prostaglandin-endoperoxide synthase 2 (prostaglandin G/H synthase and cyclooxygenase)	3.26	2.43
204802_at	NM_004165	RRAD	Ras-related associated with diabetes	21.54	7.03
204948_s_at	NM_013409	FST	Follistatin	3.91	3.18
205290_s_at	NM_001200	BMP2	Bone morphogenetic protein 2	2.28	2.00
205680_at	NM_002425	MMP10	Matrix metalloproteinase 10 (stromelysin 2)	2.79	2.18
205822_s_at	NM_002130	HMGCS1	3-hydroxy-3-methylglutaryl-Coenzyme A synthase 1 (soluble)	3.11	2.52
206211_at	NM_000450	SELE	Selectin E (endothelial adhesion molecule 1)	9.91	4.16
206463_s_at	NM_005794	DHRS2	Dehydrogenase/reductase (SDR family) member 2	33.63	41.57
206942_s_at	NM_002674	PMCH	Pro-melanin-concentrating hormone	7.95	5.09
207148_x_at	NM_016599	MYOZ2	Myozenin 2	6.87	2.54
207343_at	NM_020426	LYZL6	Lysozyme-like 6	3.62	4.81
207850_at	NM_002090	CXCL3	Chemokine (C-X-C motif) ligand 3	3.03	2.96
209189_at	BC004490	FOS	V-fos FBJ murine osteosarcoma viral oncogene homolog	5.57	13.67
209277_at	AL574096	TFPI2	Tissue factor pathway inhibitor 2	7.22	4.00
209278_s_at	L27624	TFPI2	Tissue factor pathway inhibitor 2	5.24	3.25
209419_at	AB023200	C22orf19	Chromosome 22 open reading frame 19	4.64	3.04
209774_x_at	M57731	CXCL2	Chemokine (C-X-C motif) ligand 2	2.71	2.60
209785_s_at	AF065214	PLA2G4C	Phospholipase A2, group IVC (cytosolic, calcium-independent)	2.99	2.98
209795_at	L07555	CD69	CD69 antigen (p60, early T-cell activation antigen)	2.03	2.32
210139_s_at	L03203	PMP22	Peripheral myelin protein 22	2.28	2.07

210511_s_at	M13436	INHBA	Inhibin, β A (activin A, activin AB α polypeptide)	2.37	2.81
210675_s_at	U77917	PTPRR	Protein tyrosine phosphatase, receptor type, R	2.18	2.97
211123_at	D87920	SLC5A5	Solute carrier family 5 (sodium iodide symporter), member 5	2.19	2.11
213355_at	AI989567	SIAT10	ST3 β-galactoside α-2,3-sialyltransferase 6	3.45	2.02
213375_s_at	N80918	CG018		2.39	2.13
213782_s_at	BF939176	MYOZ2	Myozenin 2	2.02	3.09
214079_at	AK000345	DHRS2	Dehydrogenase/reductase (SDR family) member 2	20.09	77.60
214321_at	BF440025	NOV	Nephroblastoma overexpressed gene	32.32	5.05
215430_at	AA757089	GK2	Glycerol kinase 2	6.27	12.75
216598_s_at	S69738	CCL2	Chemokine (C-C motif) ligand 2	5.33	4.31
217054_at	AF007194	MUC3B	Mucin 3B	11.59	2.65
217589_at	AW300309	RAB40A	RAB40A, member RAS oncogene family	7.51	3.55
219368_at	NM_021963	NAP1L2	Nucleosome assembly protein 1-like 2	5.99	2.12
219468_s_at	NM_017949	CUEDC1	CUE domain containing 1	2.53	2.11
220014_at	NM_016644	LOC51334		2.31	24.75
220116_at	NM_021614	KCNN2	Potassium intermediate/small conductance calcium-activated channel, subfamily N, member 2	2.75	9.52
220243_at	NM_014155	HSPC063	BTB (POZ) domain containing 15	3.40	3.93
220266_s_at	NM_004235	KLF4	Kruppel-like factor 4 (gut)	2.18	3.64
220542_s_at	NM_016583	PLUNC	Palate, lung and nasal epithelium carcinoma associated	2.18	2.08
221524_s_at	AF272036	RRAGD	Ras-related GTP binding D	4.80	8.50
221555_x_at	AU145941	CDC14B	CDC14 cell division cycle 14 homolog B (S. cerevisiae)	3.04	2.05
221750_at	BG035985	HMGCS1	3-hydroxy-3-methylglutaryl-Coenzyme A synthase 1 (soluble)	2.18	2.15
33304_at	U88964	ISG20	Interferon stimulated gene 20 kDa	2.12	2.01
222486_s_at	AF060152	ADAMTS1	A disintegrin-like and metalloprotease (reprolysin type) with thrombospondin type 1 motif, 1	3.37	2.27
226632_at	AL513673	CYGB	Cytoglobin	2.24	2.05
226731_at	AA156873	PELO	Pelota homolog (Drosophila)	9.41	4.61
226847_at	BF438173	FST	Follistatin	4.32	4.77
226991_at	AA489681	NFATC2	Nuclear factor of activated T-cells, cytoplasmic, calcineurin-dependent 2	3.10	2.04
227140_at	AI343467	INHBA	Inhibin, beta A (activin A, activin AB alpha polypeptide)	2.07	2.17
228038_at	AI669815	SOX2	SRY (sex determining region Y)-box 2	2.23	2.07
230657_at	AI423466	CLOCK	Clock homolog (mouse)	2.29	11.50
230966_at	AI859620	NUP62	Nucleoporin 62kDa	6.24	2.46
231042_s_at	AA809487	CAMK2D	Calcium/calmodulin-dependent protein kinase (CaM kinase) II delta	2.97	2.13
233615_at	AU157698	CGA	Glycoprotein hormones, alpha polypeptide	3.83	4.11
235652_at	AI431345	SCML1	Sex comb on midleg-like 1 (Drosophila)	3.21	22.28
237885_at	AW589793	SOX21	SRY (sex determining region Y)-box 21	10.16	12.97
239998_at	AI990484	C10orf53	Chromosome 10 open reading frame 53	4.23	2.49
240156_at	AA417099	RFX2	Regulatory factor X, 2 (influences HLA class II expression)	5.11	3.05
240793_at	BF224054	TTN	Titin	2.60	4.25
242593_at	AI833186	KIAA0143		5.33	3.38
242792_at	AA004487	NFIB	Nuclear factor I/B	2.60	2.34
244056_at	AW293443	UNQ541		12.21	13.96
244684_at	AI432340	PGGT1B	Protein geranylgeranyltransferase type I, beta subunit	9.05	8.77
1553157_at	AB055703	LHX4	LIM homeobox 4	11.17	4.64
1553428_at	NM_173675	FLJ33708		14.17	14.84
1554514_at	BC013753	FLJ20581		21.23	6.46
1554569_a_at	BC036391	CUGBP2	CUG triplet repeat, RNA binding protein 2	2.18	3.27
1554741_s_at	AF523265	FLJ30435		11.89	2.43
1554804_a_at	BC030524	CLDN19	Claudin 19	2.05	4.42
1554997_a_at	AY151286	PTGS2	Prostaglandin-endoperoxide synthase 2 (prostaglandin G/H synthase and cyclooxygenase)	4.34	2.94
1556773_at	M31157	PTHLH	Parathyroid hormone-like hormone	3.67	2.85
1559121_s_at	AI767566	ARIH2	Ariadne homolog 2 (Drosophila)	2.07	2.36
1561589_a_at	AB053319	NBEAL1	Neurobeachin-like 1	7.70	2.20
1568589_at	AF113014	C10orf74	Chromosome 10 open reading frame 74	7.61	12.19
1570022_at	BC038182	C3orf1	Chromosome 3 open reading frame 1	2.14	23.82

Ratio 1: CB100,24h-1/Control1; Ratio 2: CB100,24h-2/Control2.

of endothelial gap junctions were examined. CB (100 μg/ml, 24 h) significantly inhibited the expression of connexin37 in HUVECs (Fig 8A, 20.8±7.4% inhibition, n=6, p<0.05). Endothelium-derived nitric oxide (NO) is known to be anti-atherogenic and anti-thrombogenic[20] and Western blotting demonstrated that CB (100 μg/ml, 24 h) significantly suppressed eNOS expression (Fig 8B, 43.4±7.7% inhibition, n=5, p<0.01).

Microarray Analysis

We performed the microarray analysis using total RNA from HUVECs treated without or with CB (100 μg/ml, 24 h). Results from 2 independent samples are summarized in Tables 1 and 2. Hierarchical cluster analysis of differentially expressed genes is shown in Fig 9A,B. The data showed that several inflammation-related genes, including ICAM1 (intercellular adhesion molecule 1), interleukin 8, HMOX1 (heme oxygenase 1), VCAM-1, PTGS2 (prostaglandin-endoperoxide synthase 2), SELE (selectin E), and CCL2 (chemokine (C-C motif) ligand 2, also known as MCP-1), are significantly upregulated by CB (Table 1). Although changes in the gene expression level for MCP-1 (Table 1), eNOS (NOS3, mean ratio (fold)=0.8, data not shown), and connexin37 (GJA4, mean ratio (fold)=0.8, data

Table 2 List of Top 99 Probe Sets Downregulated by Carbon Black (CB) Identified on U133 Chips

Probe set ID	GenBank accession	Gene symbol	Gene name	Ratio 1 (fold)	Ratio 2 (fold)
203003_at	AL530331	MEF2D	MADS box transcription enhancer factor 2, polypeptide D (myocyte enhancer factor 2D)	0.49	0.42
203876_s_at	AI761713	MMP11	Matrix metalloproteinase 11 (stromelysin 3)	0.19	0.22
204196_x_at	NM_004571	PKNOX1	PBX/knotted 1 homeobox 1	0.45	0.31
205749_at	NM_000499	CYP1A1	Cytochrome P450, family 1, subfamily A, polypeptide 1	0.02	0.35
206679_at	NM_001163	APBA1	Amyloid beta (A4) precursor protein-binding, family A, member 1 (X11)	0.13	0.11
207045_at	NM_017667	FLJ20097		0.37	0.45
207252_at	NM_003669	INE1	Inactivation escape 1	0.33	0.42
207323_s_at	NM_002385	MBP	Myelin basic protein	0.34	0.47
209047_at	AL518391	AQP1	Aquaporin 1 (channel-forming integral protein, 28 kDa)	0.07	0.30
209841_s_at	AL442092	LRRN3	Leucine rich repeat neuronal 3	0.15	0.09
211516_at	M96651	IL5RA	Interleukin 5 receptor, alpha	0.38	0.36
211880_x_at	AF152507	PCDHGC3	Protocadherin gamma subfamily C, 3	0.33	0.13
213517_at	AW103422	PCBP2	Poly(rC) binding protein 2	0.41	0.46
213593_s_at	AW978896	TRA2A		0.38	0.47
213948_x_at	AI564838	IGSF4B	Immunoglobulin superfamily, member 4B	0.48	0.45
214184_at	AW195837	NPFF	Neuropeptide FF-amide peptide precursor	0.30	0.33
215209_at	AU143984	SEC24D	SEC24 related gene family, member D (S. cerevisiae)	0.13	0.48
215567_at	AU144919	C14orf111	Chromosome 14 open reading frame 111	0.20	0.28
215786_at	AK022170	HBXAP	Hepatitis B virus x associated protein	0.39	0.42
216147_at	AL353942	38606	Septin 11	0.20	0.41
219957_at	NM_017987	RUFY2	RUN and FYVE domain containing 2	0.43	0.36
220988_s_at	NM_030945	C1QTNF3	C1q and tumor necrosis factor related protein 3	0.31	0.45
221397_at	NM_023921	TAS2R10	Taste receptor, type 2, member 10	0.40	0.29
226655_at	BF126274	STX17	Syntaxin 17	0.43	0.42
227223_at	BE466173	RNPC2	RNA-binding region (RNP1, RRM) containing 2	0.48	0.46
228030_at	AI041522	RBM6	RNA binding motif protein 6	0.45	0.41
228173_at	AA810695	GNAS	GNAS complex locus	0.28	0.50
229193_at	AA005430	CROP		0.21	0.44
229365_at	BF475372	PPP1R3F	Protein phosphatase 1, regulatory (inhibitor) subunit 3F	0.22	0.35
229894_s_at	AI858067	RAB43	RAB43, member RAS oncogene family	0.32	0.43
229996_s_at	BF196224	PCGF5	Polycomb group ring finger 5	0.40	0.35
230562_at	R45298	MCPH1	Microcephaly, primary autosomal recessive 1	0.31	0.08
230609_at	BF510429	ENTH		0.42	0.24
231400_s_at	BE219311	TIMM22	Translocase of inner mitochondrial membrane 22 homolog (yeast)	0.48	0.42
232059_at	AI433419	DSCAML1	Down syndrome cell adhesion molecule like 1	0.34	0.08
232291_at	AA256157	C13orf25	Chromosome 13 open reading frame 25	0.22	0.36
232757_at	AV705679	MTSS1	Metastasis suppressor 1	0.23	0.35
233193_x_at	AK000455	MGC16733		0.34	0.38
233349_at	AI800481	TLK2	Tousled-like kinase 2	0.09	0.17
233637_at	AU146915	WDR42A	WD repeat domain 42A	0.41	0.37
234047_at	AK024127	SNRP70	Small nuclear ribonucleoprotein 70 kDa polypeptide (RNP antigen)	0.44	0.49
234562_x_at	AK000115	CKLFSF8	Chemokine-like factor super family 8	0.27	0.38
234859_at	AL137352	DKFZp434G0625		0.33	0.40
235926_at	AI312527	ANAPC5	Anaphase promoting complex subunit 5	0.45	0.44
235927_at	BE350122	XPO1	Exportin 1 (CRM1 homolog, yeast)	0.39	0.45
236076_at	AW241549	LOC257396		0.21	0.04
237305_at	AW450381	CDH2	Cadherin 2, type 1, N-cadherin (neuronal)	0.47	0.21
237834_at	BF062366	SNCAIP	Synuclein, α interacting protein (synphilin)	0.43	0.07
238279_x_at	BF062155	COL4A3BP	Collagen, type IV, alpha 3 (Goodpasture antigen) binding protein	0.17	0.46
238513_at	BF905445	PRRG4	Proline rich Gla (G-carboxyglutamic acid) 4 (transmembrane)	0.02	0.05
238563_at	AV762916	TPRT	Trans-prenyltransferase	0.40	0.37
238797_at	BF059582	TRIM11	Tripartite motif-containing 11	0.46	0.34
238982_at	AW665791	DENR	Density-regulated protein	0.08	0.14
239243_at	AA279654	ZNF638	Zinc finger protein 638	0.09	0.12
239441_at	AI359527	LOC284323		0.41	0.33
239448_at	AI475033	SMAD3	SMAD, mothers against DPP homolog 3 (Drosophila)	0.24	0.40
239583_x_at	BG354573	PSG4	Pregnancy specific beta-1-glycoprotein 4	0.49	0.45
239678_at	AL041224	AP1GBP1	AP1 gamma subunit binding protein 1	0.33	0.43
240008_at	AI955765	ARID1B	AT rich interactive domain 1B (SWI1-like)	0.02	0.16
240349_at	AV693202	PRKAA2	Protein kinase, AMP-activated, alpha 2 catalytic subunit	0.49	0.35
240458_at	AI242023	FAM20C	Family with sequence similarity 20, member C	0.49	0.39
240655_at	BE502785	ALCAM	Activated leukocyte cell adhesion molecule	0.08	0.46
241027_at	BE858373	OPA1	Optic atrophy 1 (autosomal dominant)	0.20	0.10
241174_at	AV647279	AP4E1	Adaptor-related protein complex 4, epsilon 1 subunit	0.47	0.07
241757_x_at	AA947051	D2LIC		0.42	0.38
241785_at	AA613520	DNAJC11	DnaJ (Hsp40) homolog, subfamily C, member 11	0.41	0.08
241977_s_at	AI634523	RAB3C	RAB3C, member RAS oncogene family	0.38	0.40
242279_at	R11494	SDFR1	Stromal cell derived factor receptor 1	0.31	0.20
242343_x_at	H57111	ZNF518	Zinc finger protein 518	0.41	0.11
242480_at	AA868356	MYST3	MYST histone acetyltransferase (monocytic leukemia) 3	0.44	0.18

242805_at	AW081636	CCNC	Cyclin C	0.40	0.36
242937_at	AV763408	FOXK2	Forkhead box K2	0.34	0.43
243198_at	AA020920	TEX9		0.27	0.29
243650_at	AI217992	PLEKHH2	Pleckstrin homology domain containing, family H (with MyTH4 domain) member 2	0.05	0.20
244778_x_at	N63691	M11S1	Membrane component, chromosome 11, surface marker 1	0.44	0.41
244803_at	AI335191	YAP	YY1 associated protein 1	0.48	0.41
1552536_at	NM_145206	VTI1A	Vesicle transport through interaction with t-SNAREs homolog 1A (yeast)	0.12	0.30
1552621_at	BQ613856	MGC13098		0.45	0.34
1552935_at	NM_152694	ZCCHC5	Zinc finger, CCHC domain containing 5	0.41	0.20
1553145_at	BC010030	FLJ39653		0.18	0.35
1553693_s_at	NM_032783	CBR4		0.41	0.39
1554328_at	BC041485	STXBP4	Syntaxin binding protein 4	0.33	0.49
1554707_at	BC034293	C9orf68	Chromosome 9 open reading frame 68	0.34	0.21
1554960_at	BC040018	MGC48998		0.44	0.48
1555878_at	AK094613	RPS24	Ribosomal protein S24	0.39	0.47
1556088_at	AK098491	RIP		0.44	0.28
1556322_a_at	AW952920	TJP4	Tight junction protein 4 (peripheral)	0.18	0.38
1557223_at	AK057533	RBPMS	RNA binding protein with multiple splicing	0.38	0.33
1557759_at	AW102805	FLJ10241		0.43	0.10
1559063_at	AL355689	C21orf63	Chromosome 21 open reading frame 63	0.31	0.31
1559691_at	BC032767	NDUFS1	NADH dehydrogenase (ubiquinone) Fe-S protein 1, 75 kDa (NADH-coenzyme Q reductase)	0.02	0.45
1559746_a_at	AK096662	FLJ90036		0.11	0.14
1560776_at	AU121725	HIP2	Huntingtin interacting protein 2	0.44	0.43
1561175_at	AK092513	LOC283482		0.08	0.43
1564272_a_at	AK098735	KLHDC1	Kelch domain containing 1	0.01	0.19
1564699_at	BC017920	C5orf4	Chromosome 5 open reading frame 4	0.01	0.04
1568627_at	BC032531	KIAA1387		0.47	0.44
1568782_at	BC027851	RP2	Retinitis pigmentosa 2 (X-linked recessive)	0.39	0.15
1569408_at	BC016012	EIF2C4	Eukaryotic translation initiation factor 2C, 4	0.07	0.10

Ratio 1: CB100,24h-1/Control1; Ratio 2: CB100,24h-2/Control2.

not shown) were in accordance with those in the protein expression level (Figs 7A,8), that of VCAM-1 (increase, Table 1) was dissociated from the change in protein expression (no difference, Fig 7B). Further validation is necessary by comparing the microarray data with quantitative reverse transcriptase-polymerase chain reaction (RNA level) and/or Western blotting (protein level) data.

Discussion

The major findings of the present study are that CB directly affects vascular ECs, causing cytotoxic injury, inflammatory responses, and inhibition of cell growth. To the best of our knowledge, this is the first demonstration of the direct effects of CB on the vascular endothelium. Novel aspects of this study include the finding that CB increases the production of the inflammatory chemokine, MCP-1, while it suppresses the expressions of gap junctions and eNOS in ECs. Although further validation is necessary, microarray analysis supports the finding that the expression of genes related vascular inflammation is upregulated by CB. Because EC injury, inflammation, and impairment of membrane integrity are closely related to the initiation of atherosclerosis[18,19] and NO is anti-atherogenic and anti-thrombogenic[20] the direct effects of nano-sized air pollution on ECs could represent one mechanism by which air pollution exacerbates atherosclerosis and ischemic heart disease (IHD).

We propose that EC injury is most likely mediated via the direct physical contact of CB with the cells, including the internalization of CB and excess autophagic vacuole formation. Because CB has minimal metallic components[21] it seems unlikely that the effects were mediated by chemical reactions. In addition to the direct effects of CB, it could also be possible that the changes were mediated secondari-

ly via cytokines and/or reactive oxygen species produced by the injured ECs. There is also a report that examined the toxic effects of several nano-materials, including metals (TiO2, SiO2, Co, Ni, polyvinyl chloride), on ECs and it showed that only Co particles had a cytotoxic effect on ECs[22] Thus it seems likely that there are variations in the effects of nano-particles and that our results could be specific to CB.

Associations between EC injury/inflammation and the development of atherosclerosis are well documented[18,19] Injury and/or denudation of ECs triggers the attachment of leukocytes to the subendothelial region and promotes transendothelial migration of cells (ie, the EC inflammatory process), initiating atherosclerosis. Platelets also readily accumulate where there are injured ECs, which may promote thrombus formation. Interestingly, our results showed that MCP-1 (ie, chemokine for leukocytes) but not VCAM-1 (leukocyte adhesion molecules), was induced by CB, suggesting a specific role of CB in the vascular inflammatory pathways. Impairment of EC growth may be related to impairment of angiogenesis, the formation of new blood vessels, from the existing vascular bed. Because angiogenesis is important for the maintenance of vascular integrity in both wound healing and the formation of collateral vessels in response to tissue ischemia[23] the present finding that CB inhibits EC growth may indicate an association with the progression of IHD.

In addition to EC injury/inflammation and inhibition of cell growth, we observed that CB suppressed the expression of connexin37 and eNOS protein in the vascular endothelium. Substantial evidence suggests altered expression of gap junctions during atherogenesis. Kwak et al demonstrated in mouse and human atheroma regions that expression of endothelial connexin37 was suppressed compared with normal aorta[24] Yeh et al[2] also reported reduced expres-
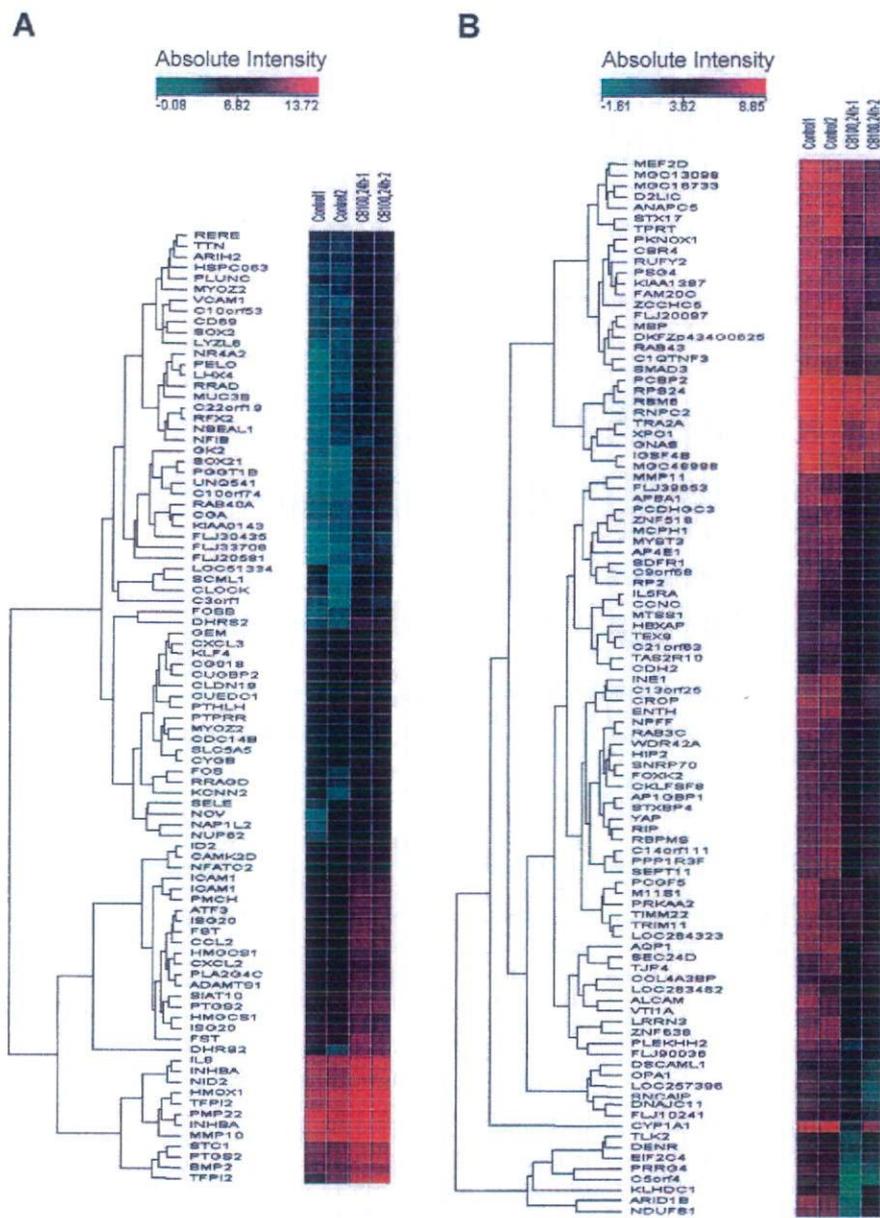
A

B

Fig 9. Hierarchical cluster analysis of differentially expressed genes (A) upregulated (top 89 genes) and (B) downregulated (top 99 genes) by carbon black (CB). Total RNA was isolated from human umbilical vein endothelial cells (HUVECs) treated without (Control) or with $100\,\mu g/ml$ CB (CB100, 24h) for 24h. Hierarchical trees were generated using Avadis Software, Version 3.3.

sion of connexin37 in the ECs of hyperlipidemic mouse aorta, and that expression recovered with simvastatin treatment.[25] ECs apparently have to physically uncouple in order to allow transendothelial migration of leukocytes. Inflammatory mediators, such as tumor necrosis factor-α[12,26] and lipopolysaccharide,[27] induce leukocyte adhesion molecules such as VCAM-1, but also downregulate connexin37 expression in vascular ECs[28,29] The inhibition of connexin37 expression by CB thus seems to be associated with EC inflammatory process such as adhesion and/or transmigration of leukocytes. Finally, a genetic polymorphism has been identified in the human connexin37 protein, apparently representing a prognostic marker for atherosclerotic plaque development.[30]

Impairment of the NO-producing function of ECs is associated with progression of atherosclerosis and IHD via several mechanisms.[31,32] For example, NO is known to inhibit platelet aggregation and thus prevent thrombus forma-

tion[20] and because it inhibits leukocyte adhesion[33] and smooth muscle proliferation,[34] NO is atheroprotective. It has recently been shown that NO regulates large artery stiffness by altering smooth muscle tone.[35] Impairment of the NO-producing function seems likely to increase cardiovascular risk factors by enhancing arterial stiffness, because a number of cardiovascular risk factors, including hypertension[36] and diabetes,[37] are associated with increased stiffness of large arteries. An example of the likely mechanism involves the induction of isolated systolic hypertension, which predominantly results from increased stiffness of large arteries, rather than elevated peripheral vascular resistance. Of note, it has been reported that EC cytotoxicity caused by organic compounds in diesel exhaust particles (DEP), including polyaromatic hydrocarbons, nitroaromatic hydrocarbons, heterocyclics, quinines, aldehydes and aliphatic hydrocarbons, was inhibited by NOS inhibitor, suggesting the involvement of peroxynitrite formation due to the organic